International Journal of Greenhouse Gas Control 114 (2022) 103593

Contents lists available at ScienceDirect

International Journal of Greenhouse Gas Control

journal homepage: www.elsevier.com/locate/ijggc

Gas switching technology: Economic attractiveness for chemical looping applications and scale up experience to 50 kW_{th}

Ambrose Ugwu [a], Carlos Arnaiz del Pozo [b], Abdelghafour Zaabout [c,*], Shareq Mohd Nazir [d], Nimet Uzun Kalendar [e], Schalk Cloete [c], Szabolcs Szima [f], Szabolcs Fogarasi [f], Felix Donat [g], Geert van Diest [h], Jan Hendrik Cloete [d], Ángel Jiménez Álvaro [b], Knuth Albertsen [h], Ana-Maria Cormos [f], Calin-Cristian Cormos [f], Shahriar Amini [i,*]

[a] Norwegian University of Science and Technology, Norway
[b] Universidad Politécnica de Madrid, Spain
[c] SINTEF Industry, Trondheim, Norway
[d] Division of Energy Processes, KTH Royal Institute of Technology, Sweden
[e] Hayat Kimya San A.Ş, Turkey
[f] Babeş-Bolyai University (UBB), Romania
[g] Laboratory of Energy Science and Engineering, ETH Zürich, Switzerland
[h] Euro Support Advanced Materials B.V, Netherlands
[i] Department of Mechanical Engineering, University of Alabama, Tuscaloosa, United States of America

ARTICLE INFO

Keywords:
Gas switching
Chemical looping
Carbon capture
Combustion
Reforming
Water splitting
Partial oxidation

ABSTRACT

Gas switching technology (GST) was introduced to facilitate operation and scale-up of pressurized chemical looping-based technologies thus bringing the expected benefits of reducing costs and energy penalty of CO_2 capture. GST has so far been applied to generate heat/power, hydrogen, syngas, and oxygen using fossil fuel gas (but also from biomass for negative CO_2 emissions) with integrated CO_2 capture at minimal energy penalty generating over 50 publication studies demonstrating the technical feasibility of the technology and quantifying the potential energy and cost savings. In contrast to conventional chemical looping, GST inherently avoids solids circulation by alternating oxidizing and reducing conditions into a single fluidized bed reactor with an oxygen carrier, thus removing many of the technical challenges that hinder the scale-up of the technology. GST has successfully been applied and demonstrated for combustion, steam/dry methane reforming, and water splitting, using different oxygen carriers, showing the ease of operation under both atmospheric and pressurized conditions and achieving high products separation efficiency.

This paper summarises the different studies completed on the Gas Switching Technology covering experimental demonstration (including the experience from a 50 kW_{th} cluster), process modelling and techno-economics, highlighting the advantages and disadvantages of the technology and discussing the way forward.

1. Introduction

Carbon Capture Utilisation and Storage (CCUS) is becoming a key component in global warming mitigation pathways, providing a set of technologies that can ensure rapid decarbonization of the energy/industrial sector and accelerated transition towards a greener economy (IEA World Energy Outlook report, 2021). CCUS technologies are developed to adapt to the different industrial requirements and are commonly categorized as post-combustion, pre-combustion, and oxy-combustion. Each of these categories gathers sets of technologies with different levels of maturity and prospects for reducing the CO_2 capture penalty/energy intensity (Abanades et al., 2015). Amongst these technologies, chemical looping has emerged as a promising technology with great prospects to reduce CO_2 capture penalty and costs (Osman et al., 2021).

Fig. 2

* Corresponding authors.
E-mail addresses: Abdelghafour.zaabout@sintef.no (A. Zaabout), samini3@ua.edu (S. Amini).

https://doi.org/10.1016/j.ijggc.2022.103593
Received 14 May 2021; Received in revised form 4 January 2022; Accepted 19 January 2022
Available online 25 January 2022

Acronyms

ACF	Annual Cash Flow
AF	Added Firing
ASU	Air Separation Unit
C	Capital
CA	CO_2 Avoidance
CC	Combined Cycle
CCReq	Equivalent Carbon Capture Ratio
CCS	Carbon Capture and Storage
COCA	Cost of CO_2 Avoidance
CSTR	Continuous Stirred Tank Reactor
GE	General Electric
GSC	Gas Switching Combustion
GSOP	Gas Switching Oxygen Production
GSR	Gas Switching Reforming
GSPOX	Gas Switching Partial Oxidation
GSWS	Gas Switching Water Splitting
GT	Gas Turbine
GT	Gas to Liquid
HAT	Humid Air Turbine
HGCU	Hot Gas Clean Up
HTW	High Temperature Winklet
IGCC	Integrated Gasification Combined Cycle
LCOE	Levelized Cost of Electricity
LCOH	Levelized Cost of Hydrogen
LHV	Lower Heating Value
MAWGS	Membrane Assisted Water Gas Shift
MDEA	Methyldiethanolamine
MEA	Monoethanolamine
OPPC	Oxygen Production Pre-combustion
PCC	Pre-combustion Capture
POX	Partial oxidation
NG	Natural Gas
NGCC	Natural Gas Combined Cycle
SMR	Steam Methane Reforming
WGS	Water Gas Shift

List of Symbols

E	Specific emissions ($kgCO_2$/unit of product)
F	Molar flow (mol/s)
Q	Heat (kW)
P	Pressure (Pa)
R	Global Reaction rate (mol/s)
R_g	Gas constant (J/molK)
T	Temperature (K)
$\dot{W}$	Power (kW)
$\dot{m}$	Mass flow (kg/s)
n	Moles (mol)
$\Delta H_{r,T}$	Enthalpy of reaction (J/mol)
t	Time (s)
y	Mole fraction (-)
υ	Stoichiometric coefficient (-)
ϕ	Capacity factor
c_p	Specific heat capacity (J/molK)

Subscripts/Superscripts

k	Component
r	Reaction
in	Inlet
out	Outlet
eq	Equilibrium
ref	Reference

1.1. Chemical looping technology

Chemical looping typically employs a dual Circulating Fluidized Bed (CFB) system (Fig. 1a) where a metal oxide is used as bed material to provide the oxygen/catalysis for the reaction with the fuel in an N_2-free environment (fuel reactor), thus resulting in a pure stream of CO_2 (and H_2O) ready for utilisation or storage if the concept is applied to combustion and power generation. The metal oxide that is reduced by the fuel is then transferred to a second reactor (air reactor) where it is re-oxidized before being reintroduced back to the fuel reactor for a new cycle of redox reactions. This technology has been proven to reduce the energy penalty of energy-intensive processes significantly, as the heat of the reaction could be transferred by metal oxide (oxygen carrier/catalyst) and utilized in the energy-demanding redox step. The chemical looping technology is mature and has been demonstrated in several lab and pilot plants under atmospheric conditions (Lyngfelt et al., 2019) for different applications (e.g. combustion (Lyngfelt, 2013; Adánez and Abad, 2019), reforming (Luis et al., 2009), water splitting (Voitic and Hacker, 2016)). However, a high-pressure operation is required to achieve maximal process efficiency and integration with other downstream processes, e.g. Fisher Tropsh, methanol synthesis, etc. (Adanez et al., 2012; Hamers et al., 2014).

The advancement of pressurized chemical looping technology has been slow, with only a few successful experimental demonstrations (Xiao et al., 2012; Chen et al., 2018; Zhang et al., 2014; Bischi et al., 2011), despite the proven fundamental prospects of the technology in driving down the compression cost of CO_2 capture (Fisher et al., 2012).

Pressurized chemical looping operation with the CFB based configuration is difficult because of the complexity of the interconnected reactor setup at extreme temperatures (> 900 °C) (Fig. 1a). To fulfil heat and mass balance, there is a need to precisely circulate a large amount of oxygen carrier material between the interconnected reactors, which is challenging given that each reactor vessel is pressurized independently. An instantaneous pressure imbalance between the interconnected reactors could cause instabilities in solids circulation, incomplete fuel conversion, sharp variations in temperature, and excessive leakages through the sealing devices which impacts negatively on the gas purity (due to undesired mixing of different gases) and the CO_2 capture efficiency. This could even lead to the risk of explosions in situations where highly reactive gases mix.

1.2. Gas switching technology

Several reactor configurations have been proposed as an alternative to carrying out chemical looping reactions under pressurized conditions covering fixed bed (Noorman et al., 2007) and internal circulating bed (A. Zaabout et al., 2016) where both were applied to combustion (Hamers et al., 2015; Osman et al., 2020) and reforming (Spallina et al., 2017; Osman et al., 2019) (a thorough review can be found (Osman et al., 2021)). amongst others, the Gas Switching Technology – GST has received increased focus in recent years due to the simplicity of its design. Unlike conventional chemical looping, GST utilizes a single bed reactor in which the oxidizing and reducing gases are alternated to achieve a redox reaction, hence avoiding the external circulation of the oxygen carrier particles (Fig. 1b) and the need for additional separation systems such as cyclones and loop seals; this also reduces the cost substantially and simplifies operation. GST has been demonstrated under both packed and fluidized bed conditions with several published studies covering the different applications and highlighting the strengths and drawbacks of the technologies (Osman et al., 2021; Noorman et al.,

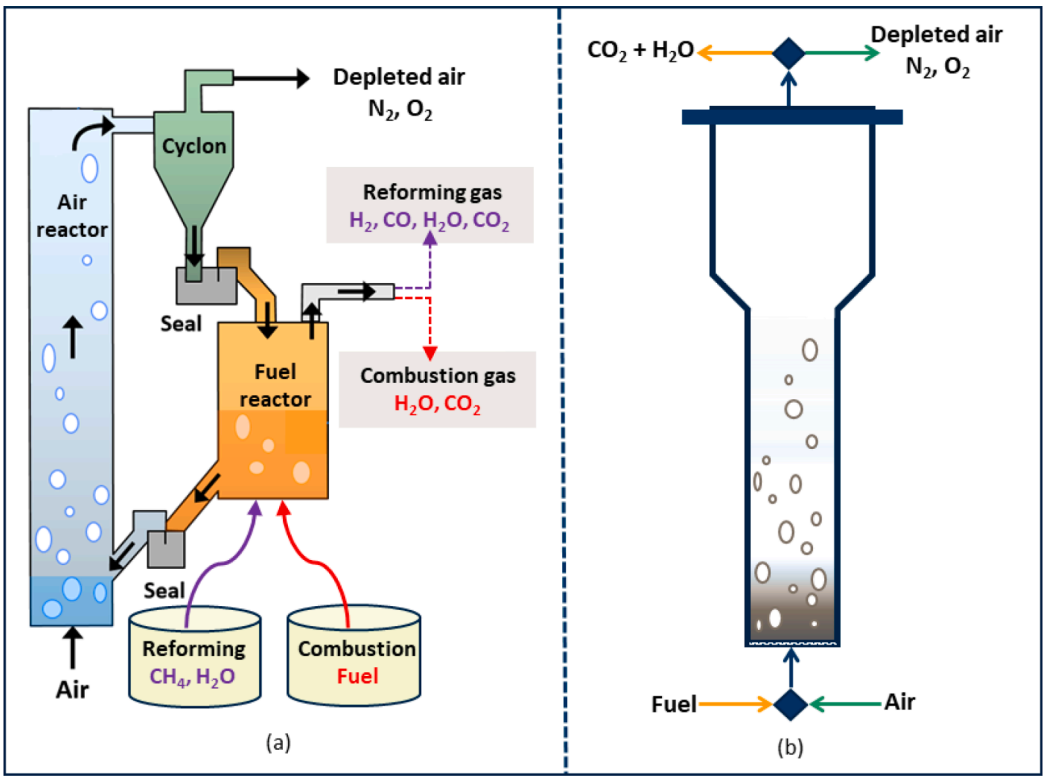

Fig. 1. Chemical looping and Gas Switching Technology for reforming and combustion applications. a) represents a scheme of conventional chemical looping reforming and combustion (Science, 2019); b) represents the simplified Gas Switching configuration of Chemical Looping Combustion (A. Zaabout et al., 2013).

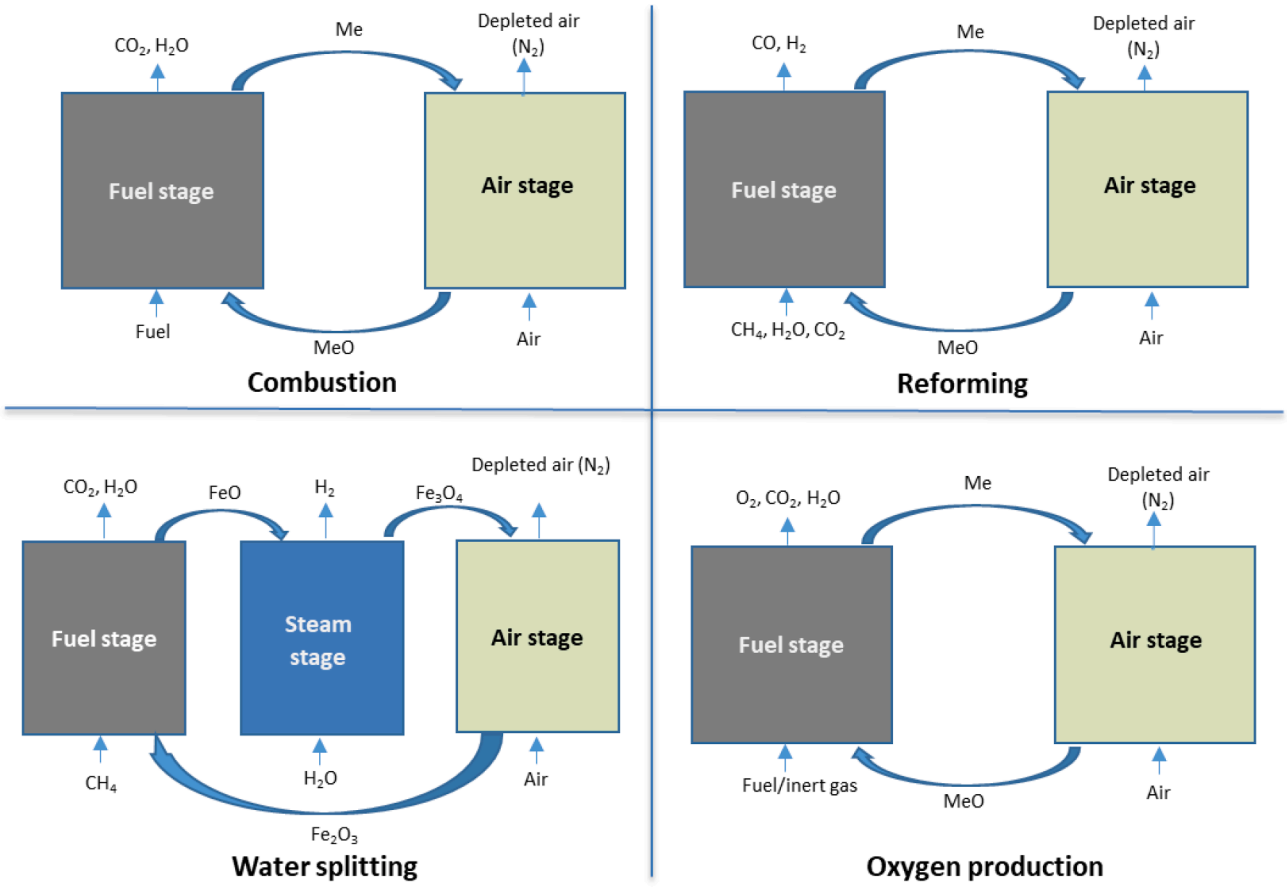

Fig. 2. The four chemical looping processes under investigation using gas switching technology.

2010). This paper focuses on the fluidized bed-based GST technology, where the oxygen carrier in the single reactor is being fluidized by the alternated feed gases. The good mixing characteristics of fluidized bed reactors bring several benefits to the process such as reduced carbon deposition (due to uniform reduction of the oxygen carrier) or reduced thermal stresses on the oxygen carrier (due to the absence of hot spots). More importantly, a wide range of inlet flowrates can be accommodated in the bubbling-turbulent fluidized bed regime, making this concept very suitable to be combined with flexible load power plants to respond to the increased share of renewable energy deployment and the associated intermittent energy supply. Process modelling, experimental demonstration, and techno-economic assessments have shown the high competitiveness of this reactor concept in addressing most shortcomings of the conventional chemical looping and demonstrated reduced costs (Cloete et al., 2016; C.A. del Pozo et al., 2019; Nazir et al., 2018; S.A. Wassie et al., 2018; C.A. del Pozo et al., 2020; S.A. Wassie et al., 2017; S. A. Wassie et al., 2018; Zaabout et al., 2017). GST has been applied to capturing CO_2 in combustion processes for heat and power generation (A. Zaabout et al., 2013; Nazir et al., 2018; Zaabout et al., 2015; ZAABOUT et al., 2021; A. Zaabout et al., 2013), H_2 production through methane reforming (S.A. Wassie et al., 2017; S.A. Wassie et al., 2018; S. A. Wassie et al., 2017; S.M. Nazir et al., 2019; A. Ugwu et al., 2019; Zaabout et al., 2019), GHG (CO_2 and CH_4) utilization through dry reforming (A. Ugwu et al., 2019), in addition to assessing its potential in providing flexibility in terms of product requirement (H_2 or power) (Szima et al., 2019).

This paper reports the nutshell of the studies completed for application of the GST technology to four processes (combustion, reforming, water splitting, and oxygen production):

- **Combustion:** Oxy-combustion of gaseous fuel using the lattice oxygen of metal oxide (oxygen carrier) to produce a pure stream of CO_2 ready for storage/further utilization. The reduced oxygen carrier is regenerated by oxidizing with air in a separate step to avoid mixing with CO_2. The hot stream of N_2 from the exothermic oxidation step is used to drive a gas turbine for power generation.
- **Reforming:** Steam/CO_2 reforming of methane to produce syngas (H_2 and CO) with integrated carbon capture. Here, the oxygen carrier does not only act as an oxygen reservoir but also as a catalyst. The overall reaction in the reduction step is endothermic, so the required heat for the process is generated in the oxidation step. Syngas production in this process can also occur through the heterogeneous partial oxidation of methane using the lattice oxygen of the metal oxide, resulting in syngas (H_2 and CO) of H_2/CO ratio ~2 suitable for Gas-to-Liquid applications (e.g. Fischer-Tropsch processes).
- **Water splitting:** Partial oxidation of a reduced oxygen carrier with steam to produce pure H_2. The oxygen carrier is first reduced by carbon-rich fuel gases and captures the CO_2 generated. After the partial oxidation of the reduced oxygen carrier with steam, the lattice oxygen is fully restored in a third reaction step by complete oxidation with air that also generates the heat needed to support the complete redox cycle.
- **Oxygen production:** The release of gaseous oxygen from metal oxides/oxygen carriers with oxygen uncoupling capability by reducing the partial pressure of oxygen at high temperatures. The oxygen carrier should have a suitable equilibrium partial pressure of gas-phase oxygen at temperatures of interest (Wang et al., 2015).

The scope of the paper covers material development, concept experimental demonstration for the four different applications, process modelling, and techno-economic for benchmarking with the state-of-the-art technologies. With the successful demonstration of the proposed gas switching technology, a business case analysis was completed for scale-up and commercialization. The demonstration challenges and learning from a 50kW$_{th}$ pre-pilot scale reactor cluster developed and commissioned to validate the feasibility of the GST concept for commercialisation is also covered. Although the GST technology was studied in different projects, the reported results are mainly focused on the outcomes of the ERA-NET GaSTech project funded by the ACT CCS call (Grant Agreement No 691,712).

2. Experimental results

2.1. Experimental demonstration

Experiments were completed in a 1 kW$_{th}$ lab-scale standalone reactor (Fig. 3) with the aim to achieve autothermal operation for each GST concept at pressurized conditions. The gas feed system consisted of gas mass flow controllers, stop and multiway valves (controlled through a LabVIEW program). Temperature and pressure sensors in the reactor setup were used for monitoring the stability of the process while the gas composition at the reactor outlet was analysed using ETG MCA 100 Syn analyser.

2.1.1. Combustion

Combustion has been one of the most extensively investigated processes of the gas switching reactor concept. Ni-based oxygen carrier was used to prove the GSC concept for power generation (A. Zaabout et al., 2013; A. Zaabout et al., 2016). Autothermal operation was achieved with CO_2 capture efficiency and CO_2 purity of 97.2% and 98.2% respectively (A. Zaabout et al., 2013). Further demonstration campaigns were completed with non-Nickel oxygen carriers as summarized in Table 1, including cheaply abundant ilmenite ore that has shown good performance even under pressurized conditions (up to 5 bar) (Zaabout et al., 2017). Another oxygen carrier with high relevance to GSC was a $CaMnO_{3-\delta}$-based oxygen carrier (developed within the EU-financed project INNOCUOUS and named "C28" (Mattisson et al., 2014), which has an exothermic reduction reaction with CO & CH_4 and has been recommended for minimizing the temperature variation across the redox cycle in order to maximize the process energy efficiency (Zaabout et al., 2015; Cloete et al., 2017). This oxygen carrier showed promising results in terms of cyclic stability even at temperatures above 900 °C and has achieved approximately 77% CH_4 conversion (Zaabout et al., 2018). However, the CO_2 capture efficiency was negatively affected by coking resulting in CO_2 emissions at the beginning of the oxidation stage when the deposited carbon combusted (see gas composition profile in Fig. 4). Based on the findings, the $CaMnO_{3-\delta}$ oxygen carrier was further optimized to reduce coking and tested in the 50kW$_{th}$ pre-pilot scale reactor as described in *Section* ***0***.

2.1.2. Reforming

Gas switching reforming is one of the extensively tested processes using the proposed gas switching reactor. The first GSR campaign was completed using NiO/Al_2O_3 oxygen carrier which has been widely studied as a good catalyst in the reduced form (Ni) for methane reforming (S.A. Wassie et al., 2017). This study successfully demonstrated autothermal operation (without an external supply of heat to drive the process) of the GSR concept where the heat for the endothermic steam methane reforming reaction was supplied by the exothermic oxidation reaction of the oxygen carrier (S.A. Wassie et al., 2017). Following the successful demonstration, Pd-based membranes have been proposed to extract H_2 during the syngas production step to improve H_2 selectivity and yield. Such integration has led to achieving CH_4 conversion of 55% at temperatures as low as 550 °C (S.A. Wassie et al., 2018). Another GSR study was completed using catalysts with reduced Nickel content (Fe-Ni/Al_2O_3, Fe-Ce/Al_2O_3) and non-Nickel content (Fe/Al_2O_3) (Zaabout et al., 2019). It was observed that Fe-Ni/Al_2O_3 performed best achieving up to 80% CH_4 conversion to syngas in the reforming stage (Zaabout et al., 2019) as shown in Fig. 5. It should be noted that CH_4 conversion deteriorates only in the last third of the reduction stage, implying that the switch to the reforming stage could be applied earlier to eliminate the large slippage of unconverted

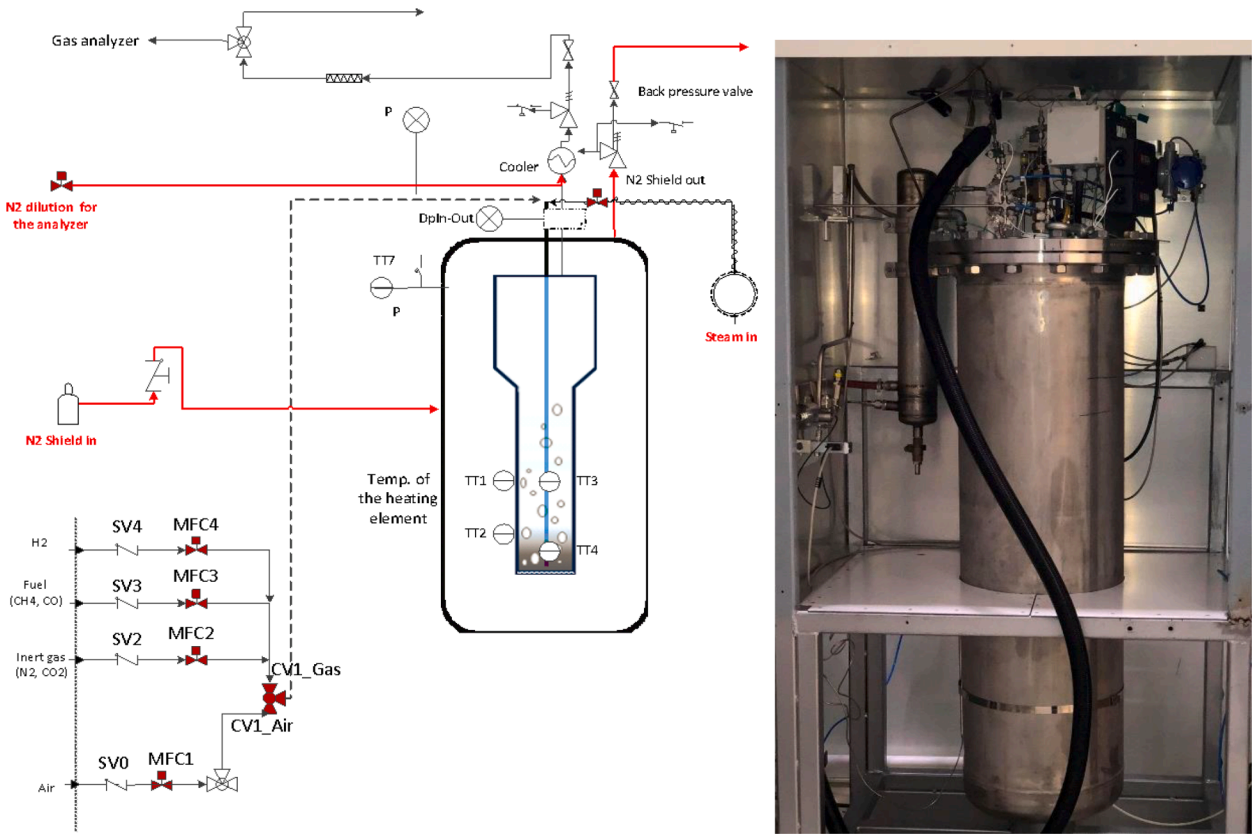

Fig. 3. Setup of the standalone pressurized fluidized bed reactor used for experimental demonstration equipped with the needed devices for gas feed and reactor monitoring.

Table 1
summary of the experimental studies completed for Gas Switching Combustion.

S/N	Title	Oxygen carrier	Condition	Findings	Ref.
1	Experimental Demonstration of a Novel Gas Switching Combustion Reactor for Power Production with Integrated CO_2 Capture	NiO/Al_2O_3 (active content 37% wt)	Temp: up to 800°C Pressure: 1 bar Fuel: CO Duration: up to 12 hr	Autothermal operation with high CO_2 capture efficiency (97.2%) and purity (98.2%)	(A. Zaabout et al., 2013)
2	Experimental demonstration of control strategies for a Gas Switching Combustion reactor for power production with integrated CO_2 capture	NiO/Al_2O_3 (active content 37% wt)	Temp: up to 600 °C Pressure: 1 bar Fuel: CO Duration: up to 12 hr	Proper heat management makes the GSC process more efficient and less energy intensive.	(A. Zaabout et al., 2016)
3	A novel gas switching combustion reactor for power production with integrated CO_2 capture: Sensitivity to the fuel and oxygen carrier types	NiO/Al_2O_3, ilmnite, Fe, $Mn(CeO_3)$	Temp: 600 - 800°C Pressure: 1.8 - 5 bar Fuel: CH_4, syngas	Complete fuel conversion with syngas. CO_2 purity (95%) and capture efficiency (97%) but lower CO_2 purity (~80%) with methane.	(Zaabout et al., 2015)
4	Autothermal operation of a pressurized Gas Switching Combustion with ilmenite ore	Ilmenite ore and NiO/Al_2O_3 (active content 37% wt)	Temperature: 680 - 920°C Pressure: 1- 5 bar Fuel: CO Duration: up to 12 hr	~85% fuel conversion (@920°C, 1 bar). Ilmenite shows good performance and enhances the attractiveness of the GSC concept	(Zaabout et al., 2017)
5	A pressurized Gas Switching Combustion reactor: Autothermal operation with a $CaMnO_{3-\delta}$-based oxygen carrier	$CaMnO_{3-\delta}$ oxygen carrier with (~4 wt%) of MgO	Temperature: 750 - 950°C Pressure: 1.8 - 5 bar Fuel: H_2 and CO Duration: up to 12 hr	~90% fuel conversion (@920°C, 1.82 bar). A power plant efficiency of 41% and CO_2 avoidance of 90% could be achieved.	(Zaabout et al., 2018)

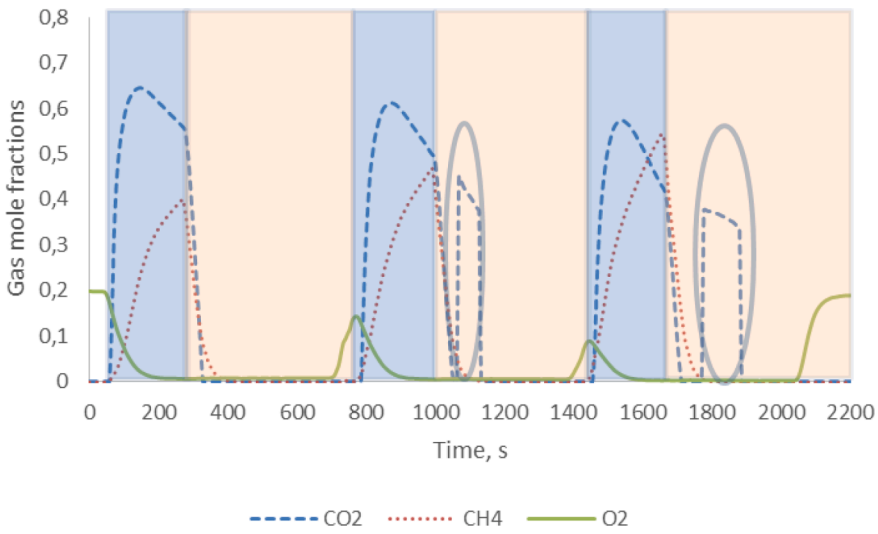

Fig. 4. Transient gas composition at the reactor outlet for three autothermal GSC cycles using CH_4 as fuel at a pressure of 1.82 bar and 880 °C. The reduction stage (where the fuel (CH_4) is supplied to combust using the lattice oxygen of the metal oxide) is in blue and the air stage (where air is supplied to re-oxidize/restore the lattice oxygen of the reduced metal oxide) is in orange (Zaabout et al., 2018).

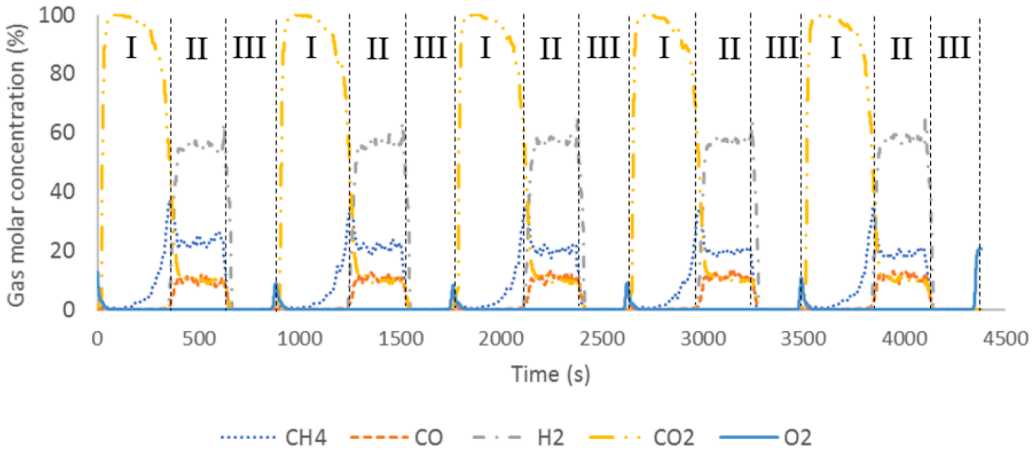

Fig. 5. The variation of the gas composition at the reactor outlet with time for five GSR cycles using Fe/Al_2O_4 at 800 °C and atmospheric pressure. The GSR stages reduction, reforming (methane and steam were fed) and oxidation with pure air are numbered respectively I, II and III (Zaabout et al., 2019).

CH_4. However, if an iron-based oxygen carrier is used, a higher reduction level is required to achieve a high conversion rate under reforming conditions, implying that the length of the reduction stage could remain as shown in the current experiments (Fig. 5). In this case, the gas products from the last third of the stage (where CH_4 conversion is low) could be fed to the proceeding reforming step. Such a process has been proven to work as shown in a previously published study (A. Ugwu et al., 2019).

The $Fe\text{-}Ni/Al_2O_3$ catalyst was investigated further at pressurized conditions up to 5 bar using a four-stage (reduction, partial oxidation, reforming, and oxidation) process to comprehensively explore the behaviour of the oxygen carrier towards syngas production[47]. The inclusion of a partial oxidation step was motivated by the fact that the performance of the reforming stage was substantially improved when the oxygen carrier was reduced more. Implying that the more the oxygen carrier is reduced, the more active sites are created for CH_4 adsorption to react with the lattice oxygen (partial oxidation of CH_4). With such a cycle, about 97.61% and 90% CH_4 conversion were achieved in the reduction and the reforming stages respectively (A. Ugwu et al., 2020). As expected from thermodynamic calculations, the CH_4 conversion decreased in the reforming stage with the increase in pressure but remained insensitive to pressure at the partial oxidation stage. Increasing the pressure also changed the mechanism for carbon deposition in the POX stage changed from methane cracking to Boudouard reaction (A. Ugwu et al., 2020) resulting in a decrease in the rate of carbon deposition at higher pressures. In general, the performance in the POX stage under pressurized conditions was better than the reforming stage in terms of CH_4 conversion and carbon of carbon deposition suggesting that eliminating the reforming stage could make the process more efficient.

Another proof of concept study was completed to demonstrate the GST concept under CO_2 (dry) reforming of CH_4 condition using Ni-based catalyst and a three-stage process as shown in Fig. 6 (A. Ugwu et al., 2019). As shown from the gas composition and the temperature profiles (Fig. 7), autothermal cycling was achieved for the range of CO_2:CH_4 ratio from 0.25 – 2 resulting in a syngas with H_2/CO molar ratio between 1 and 3 (suitable for GTL processes) with up to 90% syngas purity (A. Ugwu et al., 2019). Although carbon deposition was significant for the cases with CO_2:CH_4 ratio of less than 2, the activity and catalyst stability were not negatively affected since the cyclic nature of GSDR ensured that all the produced carbon was gasified/combusted in the preceding reforming and oxidation stages. By co-feeding, steam, CO_2 and CH_4, the combined effects of steam methane reforming and dry methane reforming was achieved with the following benefits: i) desirable syngas

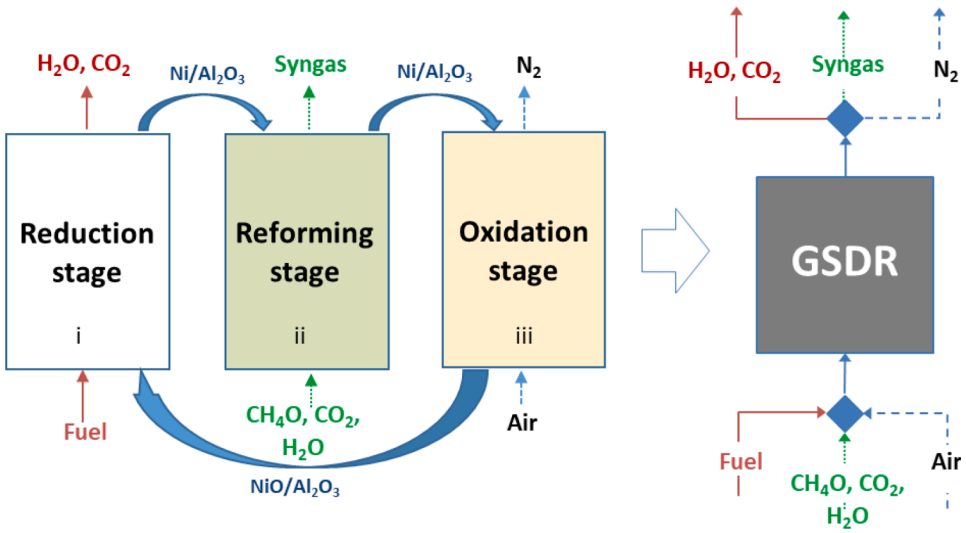

Fig. 6. The three-stage Gas switching dry reforming process design (A. Ugwu et al., 2019).

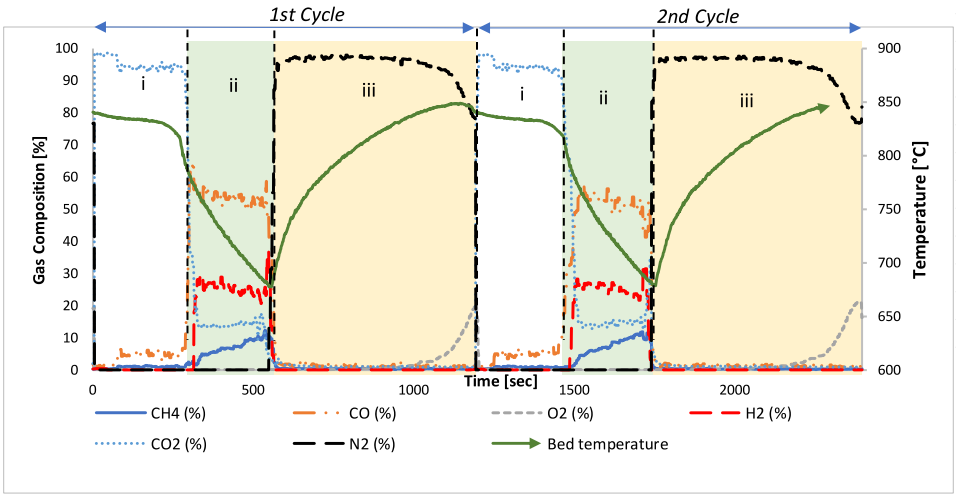

Fig. 7. The transient gas composition and temperature profile of two autothermal GSDR cycles with the target temperature to start the reduction step of 850 °C, at the atmospheric condition and CO_2/CH_4 molar ratio of 2. The reduction, reforming and oxidation stages are represented by i, ii and iii respectively (A. Ugwu et al., 2019).

quality (H_2/CO molar ratio) between 1 – 3 which could be suitable for GTL processes, ii) reduced carbon deposition and iii) reduced cost associated with air separation since ASU in the tri/autothermal reforming process is eliminated. The list of the completed gas switching reforming studies is presented in Table 2.

2.1.3. *Water splitting*

The experimental study of Gas Switching Water Splitting (GSWS) was completed using two iron-based oxygen carriers (A. Ugwu et al., 2020). The result from the first campaign using Fe_2O_3/Al_2O_3 with 35% wt active content oxygen carrier shows over 20% conversion of steam to H_2 from the transient gas composition (Fig. 8). The result also reveals that the oxygen carrier is reduced in two phases– i) the 1st phase with fuel high conversion where the oxygen carrier is reduced from Fe_2O_3 to Fe_3O_4 and ii) the 2nd phase with less fuel conversion/more fuel slippage where the oxygen carrier is reduced from Fe_3O_4 to FeO. The decrease in conversion at the 2nd phase is due to the equilibrium restriction of the reduction reaction from Fe_3O_4 to FeO. Nonetheless, the 2nd phase cannot be avoided since thermodynamics require that the oxygen carrier is reduced to at FeO/Fe to enable the splitting of H_2O to H_2 upon reoxidation, implying that GSWS will always be associated with high fuel slippage unless the gas-solid contact pattern is changed. However, the unconverted gas could be recycled to downstream processes such as combustion (A. Zaabout et al., 2013; Zaabout et al., 2015) or reforming, GSR (S.A. Wassie et al., 2018; S.A. Wassie et al., 2017), to improve process efficiency. A previous thermodynamic assessment of such integration to GSC (for IGCC power plant) shows over 4% improvement in efficiency (Cloete et al., 2015). Also, the H_2 from the steam stage could be used as fuel for combustors to raise the stream temperature to the maximum achievable turbine inlet temperature (800 - 1200 °C), ensuring high electric efficiencies, while accommodating a large amount of the unconverted fuel from the GSWS fuel stage. However, a major limitation of low H_2 purity (< 80%) due to the gas mixing while switching between the different reaction stages (Fig. 8) persisted. This problem motivated the development of Cu-doped $Mg(Fe_{0.9}Al_{0.1})_2O_4$ spinel OC with 74%wt redox-active components that result in oxygen storage capacities of ~ 10 and ~22%wt, respectively). With the higher active content of the oxygen carrier, it was expected that the GSWS stages could be longer to reduce the effect of gas mixing on the H_2 purity which happens only while changing to different process stages.

Table 2
A summary of the experimental studies completed for Gas Switching Reforming.

S/N	Title	Catalyst	Type	Condition	Findings	Ref.
1	Hydrogen production with integrated CO_2 capture in a novel gas switching reforming reactor: Proof-of-concept	NiO/Al_2O_3 (active content 35% wt)	SMR	Temp: 700 – 850 °C Pressure: 1 bar Duration: up to 72hr	Successful demonstration of autothermal GSR concept for H_2 production. Note that GSR replaces the SMR, implying that WGS and PSA steps are needed to produce pure hydrogen. However, with GSR, PSA off-gas could be used fuel stage for reducing the oxygen carrier.	(S.A. Wassie et al., 2017)
2	Hydrogen production with integrated CO_2 capture in a membrane assisted gas switching reforming reactor: Proof-of-Concept	NiO/Al_2O_3 (active content 37% wt)	Membrane assisted SMR	Temp: 440 - 550 °C Pressure: 1 - 4 bar Duration: up to 72hr	The application of Pd-based membranes for selective H_2 recovery in the reforming step has resulted in CH_4 conversion beyond equilibrium prediction (55% at 550 °C and 1.6 bar).	(S.A. Wassie et al., 2018)
3	Gas Switching Reforming (GSR) for syngas production with integrated CO_2 capture using iron-based oxygen carriers	i.Fe_2O_3/Al_2O_3 ii.Fe-Ni/Al_2O_3 iii.Fe-Ce/Al_2O_3	SMR	Temp: 700 - 850°C Pressure: 1 bar Duration: up to 72hr	Successful demonstration of autothermal GSR concept for syngas and H_2 producing using iron-based oxygen carriers. Up to 80% CH_4 conversion achieved at 800°C	(Zaabout et al., 2019)
4	The effect of gas permeation through vertical membranes on chemical switching reforming (CSR) reactor performance	N/A	N/A	Temp: 25 °C Pressure: 1 bar Duration: up to 4hr	The effect of gas extraction through vertical membranes on the bed dynamics of GSR. It was revealed that the bubble dynamics is mainly affected by the location of the membrane than the extraction rate. However, densified zone may form which could be detrimental to the process performance through causing gas channelling with associated gas bed contact.	(Wassie, 2016; S.A. Wassie et al., 2017)
5	Gas Switching Reforming for syngas production with iron-based oxygen carrier-the performance under pressurized conditions	Fe-Ni/Al_2O_3	SMR & POX	Temp: 750 - 950°C Pressure: 1- 5 bar Duration: up to 12hr	Successful demonstration of pressurized GSR concept at higher pressures up to 5 bar. The study suggested that combining SMR and POX improves gas conversion and reduces coking.	(A. Ugwu et al., 2020)
6	An advancement in CO_2 utilization through novel gas switching dry reforming	NiO/Al_2O_3 (active content 35% wt)	DMR	Temp: 750 - 950°C Pressure: 1- 5 bar Duration: up to 12hr	Autothermal operation with good CH_4 conversion to syngas of H_2/CO molar ratio suitable for GTL processes.	(A. Ugwu et al., 2019)

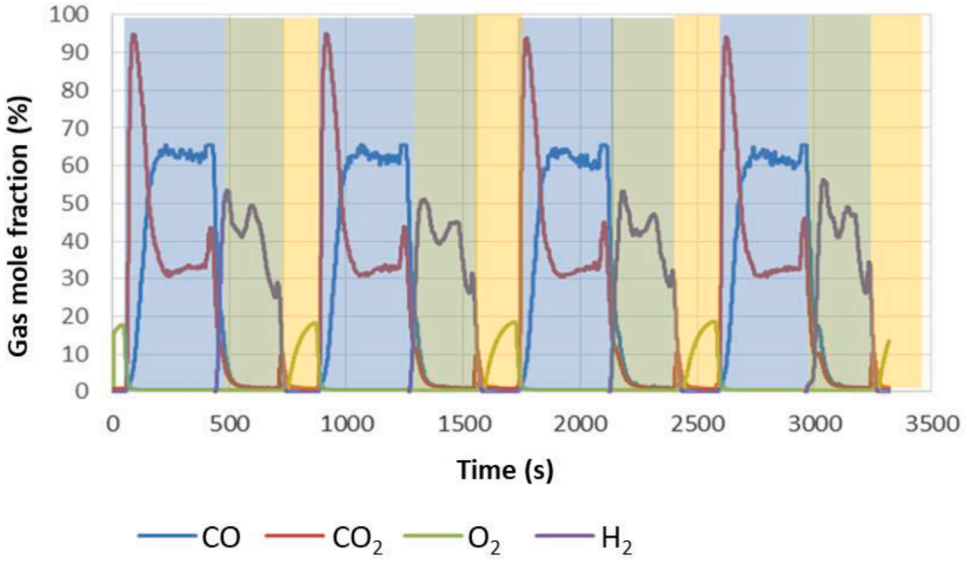

Fig. 8. The transient gas composition of 4 GSWS cycles using CO as fuel at 900 °C and 1 bar. Fuel stage in blue; Steam stage in green (H_2 production stage); Air stage in yellow (A. Ugwu et al., 2020).

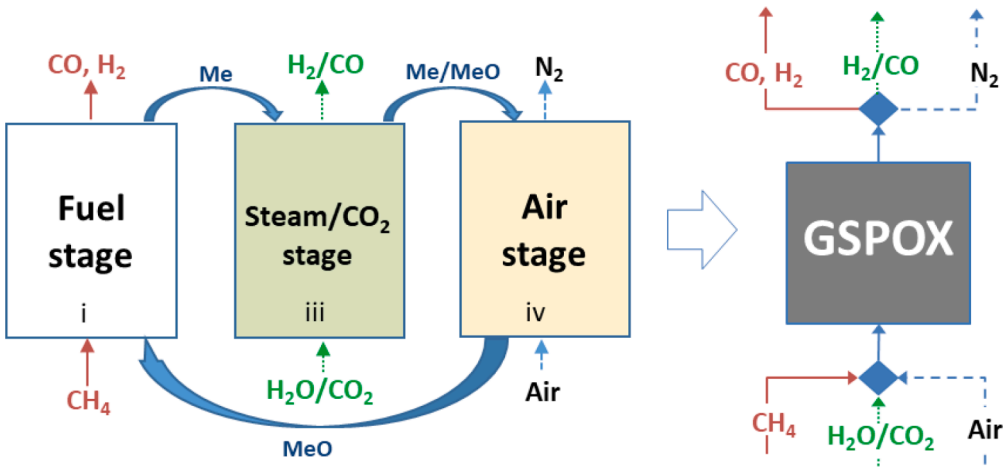

Fig. 9. Three-stage GSPOX process. i: fuel stage; ii. N_2 purge; iii: steam stage; iv: Air stage (Ugwu et al., 2021).

Although the new oxygen carrier was very reactive, it exhibited a high degree of coking and agglomeration making it difficult to be used in the reactor. In general, the proposed GSWS process is promising for H_2 production but still faced with inherent problems of thermodynamic restriction on gas conversion and the contamination of the produced H_2 due to gas mixing while switching in-between stages.

2.1.4. *Partial oxidation*

Gas switching partial oxidation is a three-step process for combined syngas and H_2/CO production (Fig. 9). This study was completed using lanthanum strontium ferrite oxygen carrier ($La_{0.8}Sr_{0.2}Fe_{0.95}Al_{0.05}O_3$) that was produced by Euro Support Advanced Materials B.V. through a spray-drying process, and the process has the capability to combine the advantages of partial oxidation of CH_4 and GSWS (*Section* ***0***) for syngas and H_2/CO production. This concept was first investigated at small scale using fluidized and packed reactors with inner diameters of 16 mm and 8 mm, respectively, (Donat and Müller, 2020; Donat et al., 2020) with a syngas H_2/CO molar ratio of ~2 achieved in the fuel stage and ~97% conversion of H_2O or CO_2 to H_2 or CO in the partial oxidation stage at atmospheric condition and temperatures above 900°C. Based on the promising result, further experiments were complete in the lab-scale standalone reactor (-Fig. 3 to understand the GSPOX behaviour on a larger scale (Ugwu et al., 2021). The result (Fig. 10) shows that the oxygen carrier exhibited high selectivity towards syngas production at the fuel stage but with some carbon deposition which was not observed in the small-scale study, probably because there the oxygen carrier was reduced more uniformly (Ugwu et al., 2021). However, the gas conversion improved and carbon deposition reduced with an increase in temperature (Ugwu et al., 2021). Co-feeding CO_2 with CH_4 at the fuel stage reduced carbon deposition significantly and improved the purity of the H_2 produced at the steam stage but also reduced the syngas H_2/CO molar ratio from 3.75 to 1 (at CO_2/CH_4 ratio of 1, 950 °C and 1 bar). Interestingly, the demonstration of CO_2 utilization at the fuel stage showed a stable syngas production over 12 h (Ugwu et al., 2021) and maintained the H_2/CO ratio at almost unity. When steam was introduced after the 12 h fuel stage, similar gas composition and temperature profile as the case with 3 mins fuel stage, suggesting that the oxygen carrier was exposed to simultaneous partial oxidation of CH_4 with the lattice oxygen which was restored instantly by the incoming CO_2 (Ugwu et al., 2021). The addition of steam increased the H_2/CO ratio and reduced carbon deposition (at the H_2O/CH_4 ratio of 1, 950 °C and 1 bar). With the flexibility that H_2O and CO_2 utilization offer in controlling syngas H_2/CO ratio and reducing coking, GSPOX could be applied to any downstream process, e.g. gas-to-liquid (GTL) processes. The

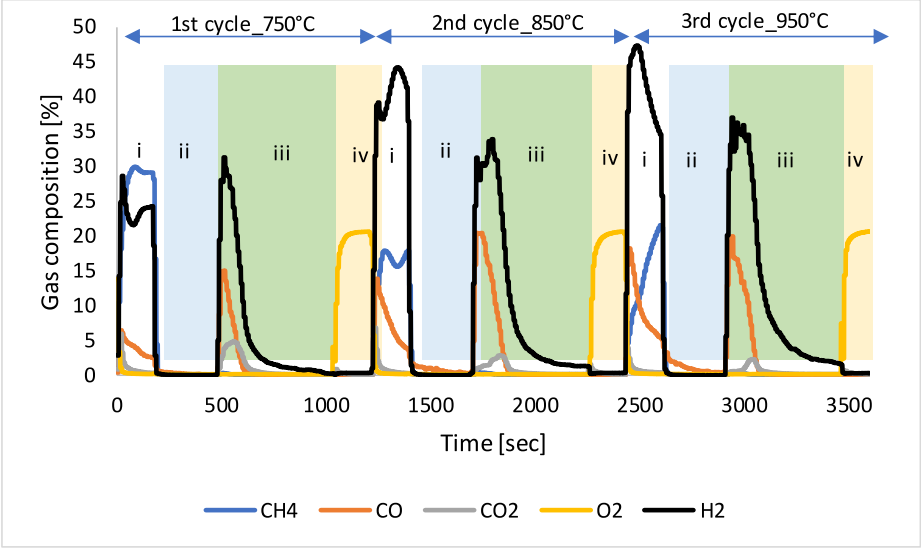

Fig. 10. The transient gas composition for three GSPOX cycles at CH_4 molar fraction of 50% diluted in N_2, 1 bar, and temperature from 750 to 950 °C. i: fuel stage; ii. N_2 purge; iii: steam stage; iv: Air stage (Ugwu et al., 2021).

high-pressure demonstration achieved over 70% fuel conversion at 5 bar and 950 °C (Ugwu et al., 2021).

2.2. Pre-pilot scale reactor cluster

As illustrated in Section 0, four GST processes (combustion, reforming, water splitting, and partial oxidation) have been successfully demonstrated in the 5 cm ID lab-scale standalone setup ((Fig. 3) which does not operate continuously. However, a continuous operation is required to realize the full potential of GST processes and make them economically viable for commercialization. Based on this, a 50kW$_{th}$ pre-pilot cluster was designed and constructed (Fig. 11) consisting of three dynamically identical reactors (10 cm ID each) that operate in an automated manner for a continuous supply of products gas to a downstream process. The reactors can withstand up to 1000 °C and 20 bar and a standpipe was designed to feed gas towards the bottom of the bed to achieve fountain-like gas distribution for good circulation of gases across the bed. The working principle of the cluster is shown in Fig. 12 where different redox steps are alternated to ensure that at least one reactor is on a given step each time to achieve pseudo-continuous operation.

Nonetheless, the major challenge of GST still remains the need for a high-temperature valve, to be placed on the reactor outlet to switch between the different stages involved in the process which was not considered in the present design (e.g. oxidation and reduction are the two stages involved when GST is applied to combustion).

2.2.1. Demonstration and learning

The $CaMnO_{3-\delta}$-based oxygen carrier (with an average particle size of 150 μm) that has been extensively tested in our previous study (Zaabout et al., 2018) was optimized to reduce coking and tested in the cluster under the combustion mode. The objective was to understand the interactions between the individual reactors in operation and implement different operational strategies for the operation of large-scale Gas Switching Technology. The target was to operate the cluster autothermally under gas switching combustion (GSC) and reforming modes at high pressures.

2.2.1.1. Combustion with methane. The first demonstration of the cluster was completed using a two-stage (reduction and oxidation) GSC process. Each reactor was loaded with 10 kg (30 kg in total) of $CaMnO_{3-\delta}$-based oxygen carrier and the combustion started at 800 °C (the reactor was heated electrically) at atmospheric pressure. Methane was used as fuel in the reduction stage while pure air was fed to oxidize the oxygen carrier. Over 80% CH_4 conversion (to CO_2 and H_2O) was achieved combined with CO_2 capture efficiency as high as 97% (indicating that carbon deposition was minimized). The fuel conversion was also observed to improve with cycling showing that the oxygen carrier requires several cycles to activate in agreement with previous studies (Zaabout et al., 2018; Hallberg et al., 2016).

Unfortunately, the oxygen carrier elutriated from the bed and formed hard agglomerates in the downstream lines, back-pressure controllers (BCPs), and the heat exchanger at the reactor outlet (Fig. 13). Particle elutriation was a challenge because the cluster was designed without an expanded freeboard to achieve compact reactors, thus particles easily attain the terminal velocity. Another challenge came from the steam produced from the combustion of CH_4 which made the particles sticky and easy to agglomerate in the lines, BCPs, and the heat exchanger. Analysis of these particles via X-ray diffraction showed that they were compositionally identical with the particles in the bed, indicating that phase segregation (e.g. of Ca-, Mg- or Mn-species) did not occur. Hence, the clogging was caused by fine oxygen carrier particles entrained from the bed in combination with moisture, which needs to be considered and prevented in future studies to ensure stable operation of the process.

2.2.1.2. GSC with co. A further experimental campaign was completed using CO as fuel instead of CH_4 (to prevent moisture in the system) at atmospheric pressure and temperatures between 800 and 900 °C. The weight of the oxygen carrier (bed) inside the reactor was also reduced from 10 kg to 7 kg (making about 50 cm bed height) to enhance uniform fluidization. The result (temperature and gas composition profiles in Fig. 14) shows several stable and repeatable cycles. Autothermal operation (without external heat supply) was achieved in each reactor using CO as fuel under atmospheric conditions. At the fuel stage, complete conversion of CO was achieved at 98.9% CO_2 capture efficiency (Fig. 14). In the oxidation stage, no CO_2/CO was observed (Fig. 14), indicating no carbon deposition during the previous fuel stage. It was ensured that the oxygen carrier was completely oxidized by monitoring the molar percentage of oxygen in the product gas until a steady-state (about 21%) was achieved. The temperature profiles at the bottom, centre, and top of the reactor bed (T1, T2 and T3 respectively) were almost identical (Fig. 14) showing that good mixing of the solid was achieved with the use of a gas-feeding lance to distribute the gases.

The result also shows that the temperatures increase in both reduction and the oxidation stages, implying that autothermal operation (without external heat supply) of the proposed GST technology is always

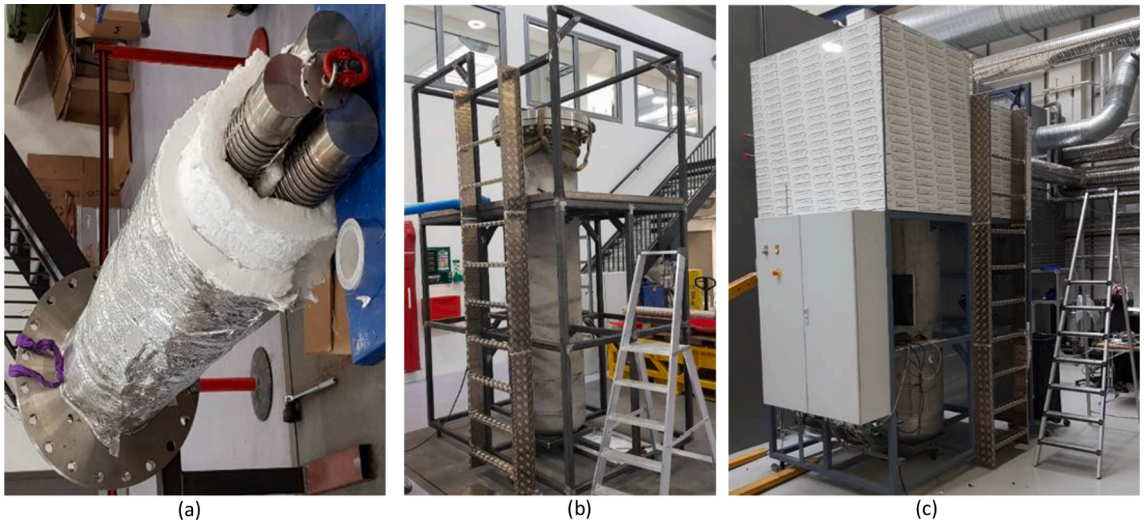

Fig. 11. Photographs of the GST reactor cluster designed to achieve continuous operation. (a) the symmetrical arrangement of the three dynamically identical reactor cluster (b)the experimental setup under construction; (d) the commissioned setup.

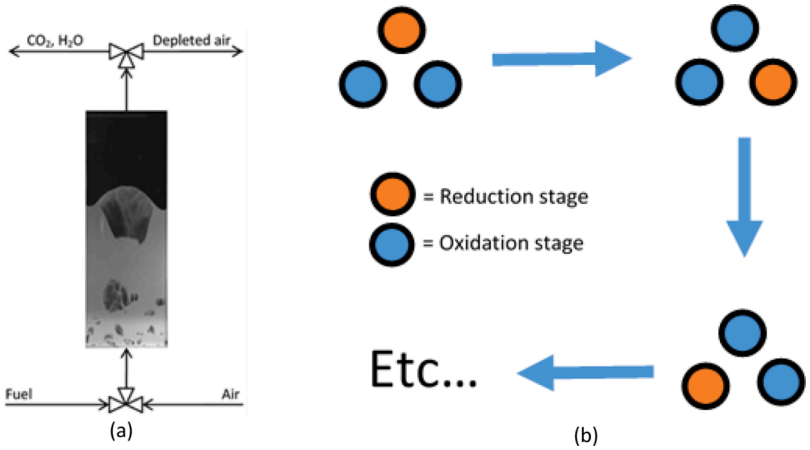

Fig. 12. a) Simple illustration of the gas switching technology under the combustion mode. b) a schematic illustration of the working principle of GST reactor cluster where each circle represents the individual reactor in a different redox step to achieve continuous operation.

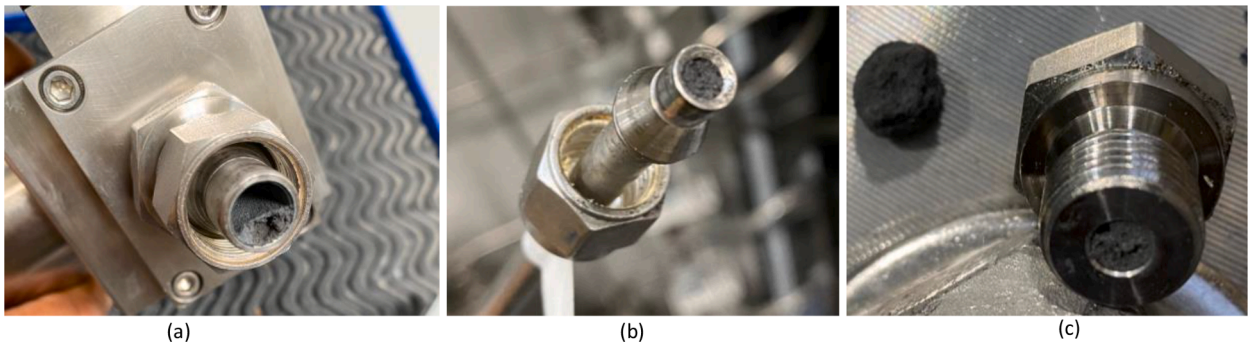

Fig. 13. (a)Clogging of the BCPs; (b) clogging of the gas outlet line; and (c) clogging of the drainage at the bottom of the heat exchanger.

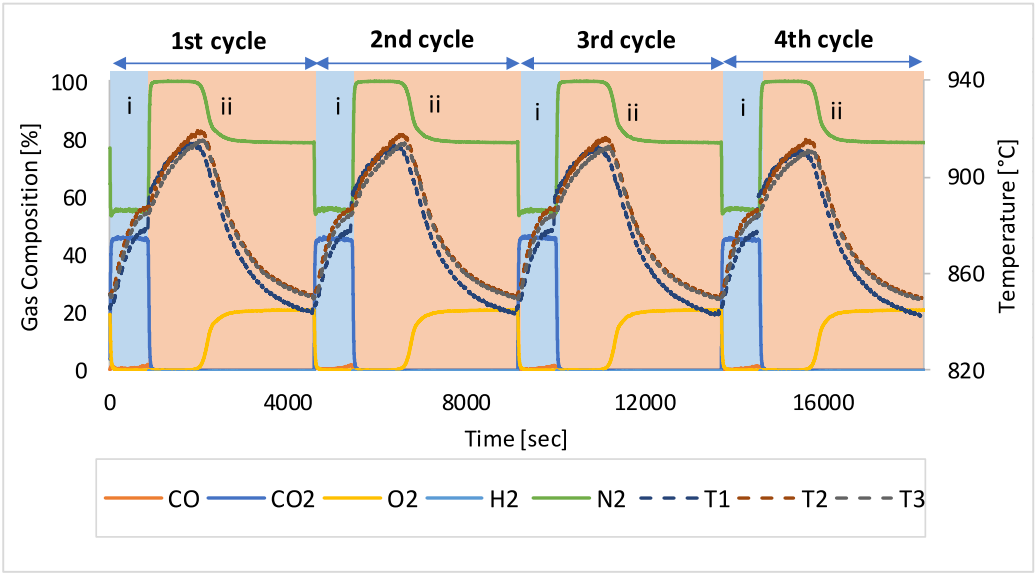

Fig. 14. The autothermal transient gas composition and temperature profile of Reactor 1 at 850 °C and 1 bar. The reduction/fuel stage is indicated as i (blue) while the oxidation stage is indicated as ii (pitch). T1, T2, and T3 are temperature measurements at the bottom, centre, and top of the bed inside the reactor. For each cycle, the flowrate at the fuel stage was as follows: CO (20nl/min) and N_2 (15nl/min) for 15 min at the reduction/fuel stage while 30nl/min of air was fed in the oxidation stage for 75 min.

feasible which can reduce the energy demand associated with CO_2 capture.

However, particle elutriation persisted and by reducing the gas flowrate (by 50%) to prevent this, part of the bed defluidized in the fuel stage. Heat and gas flow were not evenly distributed within the reactors, causing excessive reduction of part of the bed, hot spots, and melting/agglomeration of the particles. At this point, it was clear that the reactor would not be operated further in the current state and as the main challenge was particle elutriation. A possible solution could be to increase the particle size range above 150 μm but still within Geldart class B for easy fluidization. The reactor could also be modified to include an expanded freeboard which decreases gas velocity and prevent the particles from attaining the terminal velocity. Other challenges can arise from the transient nature of GST, such as the cyclic temperature

Table 3
Kinetic expressions for GS clusters.

GSC		
REDUCTION	$CH_4 + 4Fe_2O_3 \rightarrow 8FeO + CO_2 + 2H_2O$	$R_1 = \frac{1}{\tau} n_{CH_4} n_{Fe_2O_3}$
	$H_2 + Fe_2O_3 \rightarrow 2FeO + H_2O$	$R_2 = \frac{1}{\tau} n_{H_2} n_{Fe_2O_3}$
	$CO + Fe_2O_3 \rightarrow 2FeO + CO_2$	$R_3 = \frac{1}{\tau} n_{CO} n_{Fe_2O_3}$
OXIDATION	$O_2 + 4FeO \rightarrow 2Fe_2O_3$	$R_4 = \frac{1}{\tau} n_{O_2} n_{FeO}$
GSR		
REDUCTION	$CH_4 + 4NiO \rightarrow 4Ni + CO_2 + 2H_2O$	$R_1 = \frac{1}{\tau} n_{CH_4} n_{NiO}$
	$H_2 + NiO \rightarrow Ni + H_2O$	$R_2 = \frac{1}{\tau} n_{H_2} n_{NiO}$
	$CO + NiO \rightarrow Ni + CO_2$	$R_3 = \frac{1}{\tau} n_{CO} n_{NiO}$
OXIDATION	$O_2 + 2Ni \rightarrow 2NiO$	$R_4 = \frac{1}{\tau} n_{O_2} n_{Ni}$
REFORMING	$CH_4 + H_2O \leftrightarrow CO + 3H_2$	$R_5 = \frac{1}{\tau}\left(p_{CH_4} p_{H_2O} - \frac{p_{CO} p_{H_2}^3}{K_{SMR}}\right)$
	$CO + H_2O \leftrightarrow CO_2 + H_2O$	$R_6 = \frac{1}{\tau}\left(p_{CO} p_{H_2O} - \frac{p_{CO_2} p_{H_2O}}{K_{WGS}}\right)$
GSPOX		
PARTIAL OXIDATION	$CH_4 + 0.74XO_{1.35} \rightarrow 0.74X + CO + 2H_2$	$R_1 = \frac{1}{\tau} n_{CH_4} n_{XO}$
	$0.74X + CO_2 \leftrightarrow 0.74XO_{1.35} + CO$	$R_2 = \frac{1}{\tau}(y_{CO_2} - y_{CO_2,eq}) n_{gas} n_X$
	$0.74X + H_2O \leftrightarrow 0.74XO_{1.35} + H_2$	$R_3 = \frac{1}{\tau}(y_{H_2O} - y_{H_2O,eq}) n_{gas} n_X$
OXIDATION	$1.48X + O_2 \rightarrow 1.48XO_{1.35}$	$R_1 = \frac{1}{\tau} n_{O_2} n_X$
REDUCTION	$0.74XO_{1.35} + H_2 \rightarrow 0.74X + H_2O$	$R_1 = \frac{1}{\tau} n_{H_2} n_{XO}$
	$0.74XO_{1.35} + CO \rightarrow 0.74X + CO_2$	$R_2 = \frac{1}{\tau} n_{CO} n_{XO}$
	$CH_4 + 2.96XO_{1.35} \rightarrow 2.96X + CO_2 + 2H_2O$	$R_3 = \frac{1}{\tau} n_{CH_4} n_{XO}$
GSOP		
REDUCTION	$CH_4 + 8Ca_2AlMnO_{5.5} \rightarrow 8Ca_2AlMnO_5 + CO_2 + 2H_2O$	$R_1 = \frac{1}{\tau} n_{CH_4} n_{Ca_2AlMnO_{5.5}}$
	$H_2 + 2Ca_2AlMnO_{5.5} \rightarrow 2Ca_2AlMnO_5 + H_2O$	$R_2 = \frac{1}{\tau} n_{H_2} n_{Ca_2AlMnO_{5.5}}$
	$CO + 2Ca_2AlMnO_{5.5} \rightarrow 2Ca_2AlMnO_5 + CO_2$	$R_3 = \frac{1}{\tau} n_{CO} n_{Ca_2AlMnO_{5.5}}$
OXIDATION	$O_2 + 8Ca_2AlMnO_5 \leftrightarrow 8Ca_2AlMnO_{5.5}$	$R_4 = \frac{1}{\tau}(y_{O_2} - y_{O_{2,eq}}) \times n_{gas} n_{s,\ reactant}$
GSWS		
REDUCTION & WATER SPLITTING	$CH_4 + 12Fe_2O_3 \rightarrow 8Fe_3O_4 + CO_2 + 2H_2O$	$R_1 = \frac{1}{\tau} n_{CH_4} n_{Fe_2O_3}$
	$H_2 + 3Fe_2O_3 \rightarrow 2Fe_3O_4 + H_2O$	$R_2 = \frac{1}{\tau} n_{H_2} n_{Fe_2O_3}$
	$CO + 3Fe_2O_3 \rightarrow 2Fe_3O_4 + CO_2$	$R_3 = \frac{1}{\tau} n_{CO} n_{Fe_2O_3}$
	$CH_4 + 4Fe_3O_4 \rightarrow 12FeO + CO_2 + 2H_2O$	$R_4 = \frac{1}{\tau} n_{CH_4} n_{Fe_3O_4}$
	$H_2 + Fe_3O_4 \leftrightarrow 3FeO + H_2O$	$R_5 = \frac{1}{\tau}(y_{H_2} - y_{H_{2,eq}}) n_{gas} n_{s,react}$
	$CO + Fe_3O_4 \leftrightarrow 3FeO + CO_2$	$R_6 = \frac{1}{\tau}(y_{CO} - y_{CO,eq}) n_{gas} n_{s,react}$
OXIDATION	$O_2 + 6FeO \rightarrow 2Fe_3O_4$	$R_7 = \frac{1}{\tau} n_{O_2} n_{FeO}$
	$O_2 + 4Fe_3O_4 \rightarrow 6Fe_2O_3$	$R_8 = \frac{1}{\tau} n_{O_2} n_{Fe_3O_4}$

variation imposing thermal stress on the oxygen carrier but this challenge can be successfully minimized through heat management strategies as illustrated in a previous study (Cloete et al., 2017).

3. Large scale process techno-economic assessment

The assessment of promising oxygen carriers for each gas switching technology required the adoption of several modelling simplifications with regards to reactor performance and process simulation. The following sections will discuss the assumptions and modelling approach undertaken for the process synthesis of novel power and H_2 production plants, as well as the key findings and results.

3.1. Reactor modelling

The dynamic operation of a gas switching cluster was modelled in equation-orientated software (Matlab, Scilab) to determine the instantaneous outlet stream details of each step in the cycle. This involves the solving of the mass and energy balance (*Eq. (1)*, *Eq. (2)*) for each reactor and the subsequent blending of the outlet streams from each step to send a uniform stream to downstream process units. For each oxygen carrier type, specific kinetic expressions were used.

$$\frac{dn_k}{dt} = F_{in} y_{in,k} + F_{out} y_{out,k} + \sum_{r=1}^{R} \upsilon_{r,k} R_r \tag{1}$$

Table 4
Equilibrium constants and mole fractions.

Cluster	Item	Ref
GSR	K_{SMR}, K_{WGS}	(Xu and Froment, 1989)
GSPOX	$\frac{y_{H_2}}{y_{H_2}+y_{H_2O,eq}} = 0.95$ $\frac{y_{co}}{y_{co}+y_{co_2,eq}} = 0.95$	
GSOP	$y_{O_2,eq} = \frac{1}{P}\exp\left(\frac{-91,000}{R_g}\left(\frac{1}{T}-\frac{1}{873.15}\right)\right)$	(Larring et al., 2017)
GSWS	$\frac{y_{H_2,eq}}{y_{H_2,eq}+y_{H_2O}} = 1.847 \times 10^{-6}T^2 - 5.181 \times 10^{-3}T + 3.798$ $\frac{y_{CO,eq}}{y_{CO,eq}+y_{CO_2}} = 5.163 \times 10^{-7}T^2 - 1.517 \times 10^{-3}T + 1.376$	(Rydén and Arjmand, 2012)

$$\frac{dT}{dt} = \frac{-F_{in}\sum_k y_{in,k}\int_{T_{in}}^{T} c_{p,k}dT + \sum_{r=1}^{R}\xi_r\left(-\Delta H_{r,T}\right)}{\sum_k n_k c_{p,k}} \quad (2)$$

The reactors were operated under fluidized conditions, attaining homogenous temperature and composition distributions across the bed. The reactor was modelled as a Continuous Stirred Tank Reactor (CSTR), with full oxygen carrier reactivity (no fuel slip), given the high mixing properties of large-scale fluidized beds (A. Zaabout et al., 2013). High kinetic rates were imposed through a small relaxation time constant ($\tau = 0.01$) to ensure that either equilibrium conversion or complete conversion of the reactants was reached[32, 36]. Detailed kinetic and equilibrium expressions for each GS technology are presented in Table 3 and Table 4 in the Appendix, respectively. For heterogenous gas-solid reactions, the kinetic law is dependant on the number of moles of the gaseous species, i.e., proportional to pressure assuming an ideal gas law, while for the homogeneous gas-gas reactions, the effect of operating pressure is determined by the stoichiometry of the reaction, following the Le Châtelier principle.

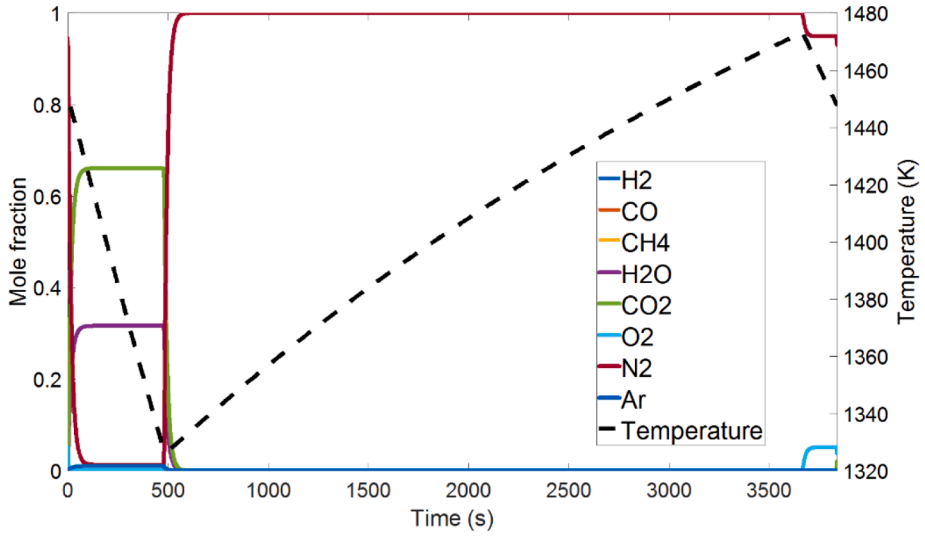

Fig. 15. Reactor outlet gas species composition and temperature plot over one complete GSC cycle. In the first 480 s the oxygen carrier is reduced by fuel, whereas for the remainder of the process the oxygen carrier is oxidised by a depleted air stream.

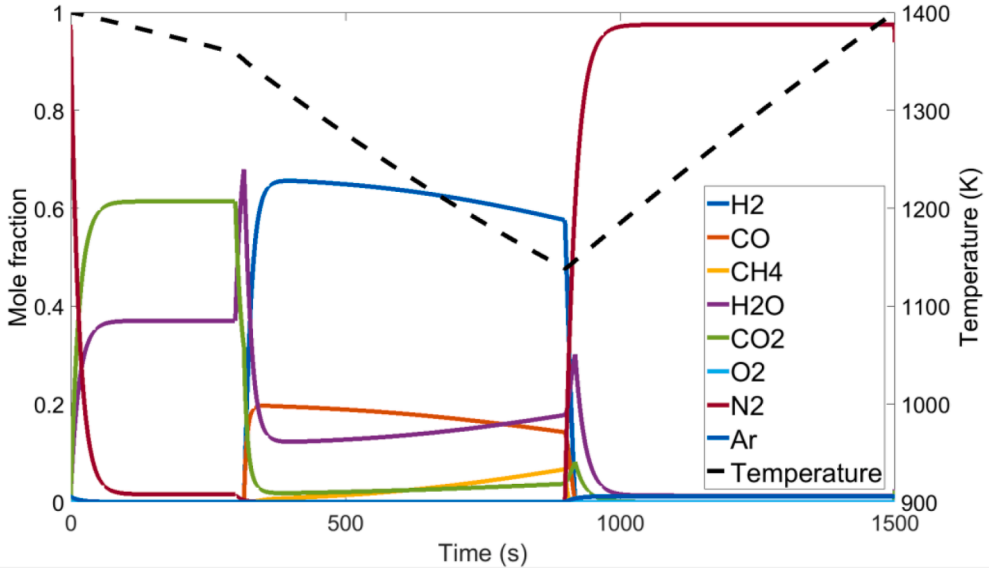

Fig. 16. Reactor outlet gas species composition and temperature plot over one complete GSR cycle. The first 300 s of the cycle is reduction with PSA off-gas fuel, followed by 600 s of steam-methane reforming and 600 s of oxidation with air (S.M. Nazir et al., 2019).

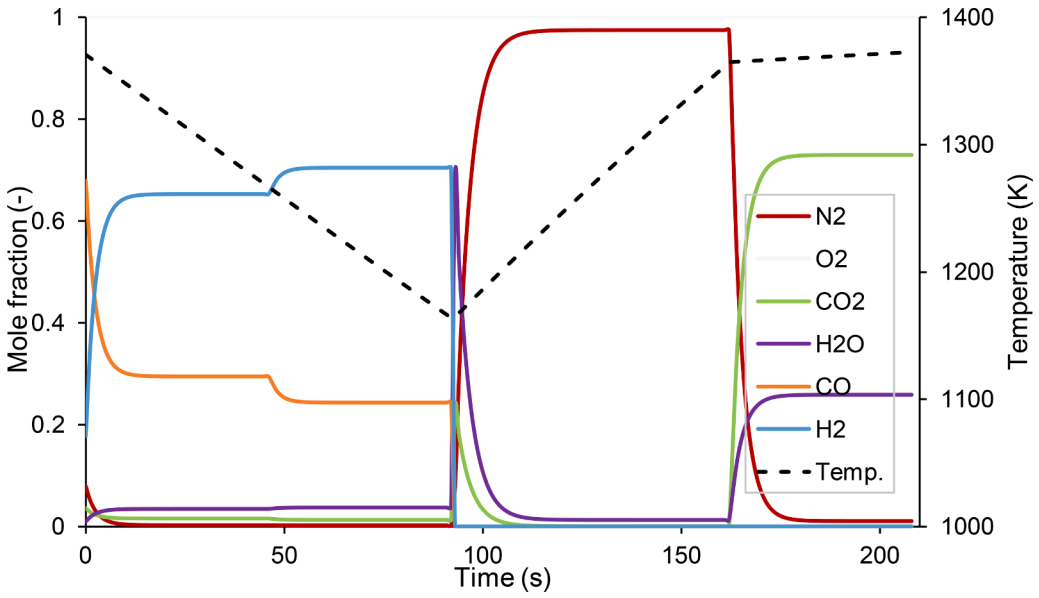

Fig. 17. Reactor outlet gas species composition and temperature plot over a complete GSPOX cycle. The first 96 s is the partial oxidation of the fuel, oxidation step takes place until 162 s, followed by a reduction step 208 s.

3.1.1. *Combustion*

The Gas Switching Combustion (GSC) technology was studied in detail as it composed the main building block of the novel power plant models from solid fuels with inherent CO_2 capture. A GSC cycle is presented in Fig. 15. The oxygen carriers employed were Nickel and Ilmenite, with a formulation taken from (Abad et al., 2007). In combustion, a syngas fuel is introduced in the reduction step where it becomes fully combusted to H_2O and CO_2. In the oxidation step, an air stream re-oxidises the carrier and heats up. The oxygen-depleted outlet is subsequently integrated into a power cycle. A maximum reactor temperature of 1200 °C is considered in the studies. The results of the experimental demonstration Section **0** show the temperature was much lower, but this was because the oxidation step was not stopped after the temperature at the maximum reactor temperature, so the potential for much higher temperatures was not exploited. The average oxidation step outlet temperature was maximized through optimal heat management strategies (A. Zaabout et al., 2016; Cloete et al., 2015), as it is a critical factor to reach attractive thermal efficiencies (C.A. del Pozo et al., 2019).

3.1.2. *Reforming*

Gas Switching Reforming utilizes a natural gas feedstock with steam to carry out its reforming with pure Nickel acting as a catalyst. A syngas with a H_2 to CO ratio of 3 is obtained at the outlet, achieving high methane conversion due to the high reactor temperature relative to fired tubular reforming. After the reforming step, the oxygen carrier reacts with an air stream until 30% of the carrier is oxidised. Subsequently, it is reduced with low heating value PSA off-gases in the reduction step, before the reforming step. A conservative maximum reactor temperature of 1100 °C was assumed to increase the robustness of the concepts evaluated. Furthermore, cases with thermal mass (steel rods) in the reactor volume allowed for a smaller temperature variation across the

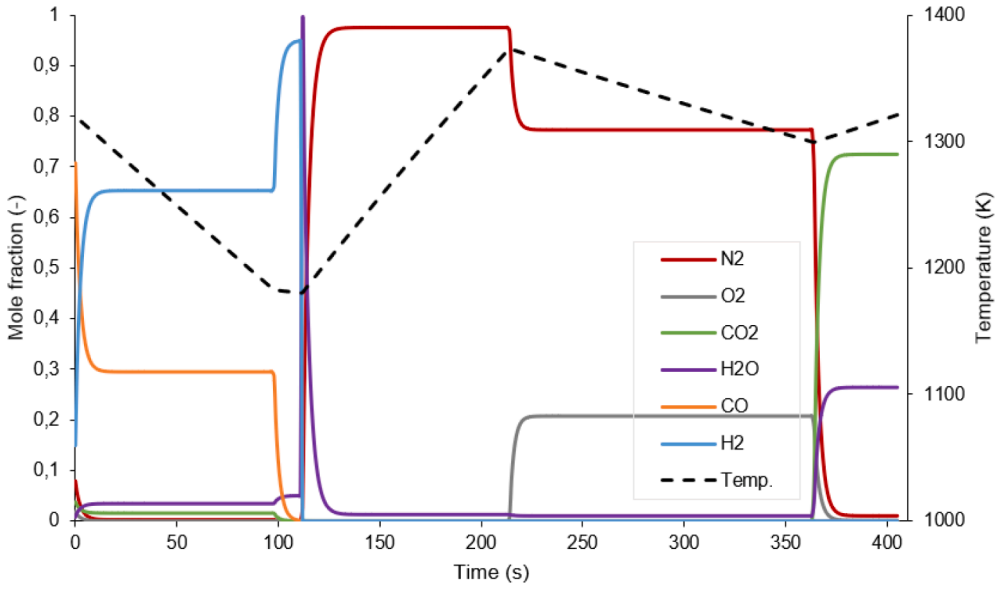

Fig. 18. Reactor outlet gas species composition and temperature plot over a complete GSPOX cycle with water splitting. The first 98 s is the partial oxidation of the fuel, followed by water splitting until 112 s, while a long oxidation step takes place until 363 s, followed by a reduction step 405 s.

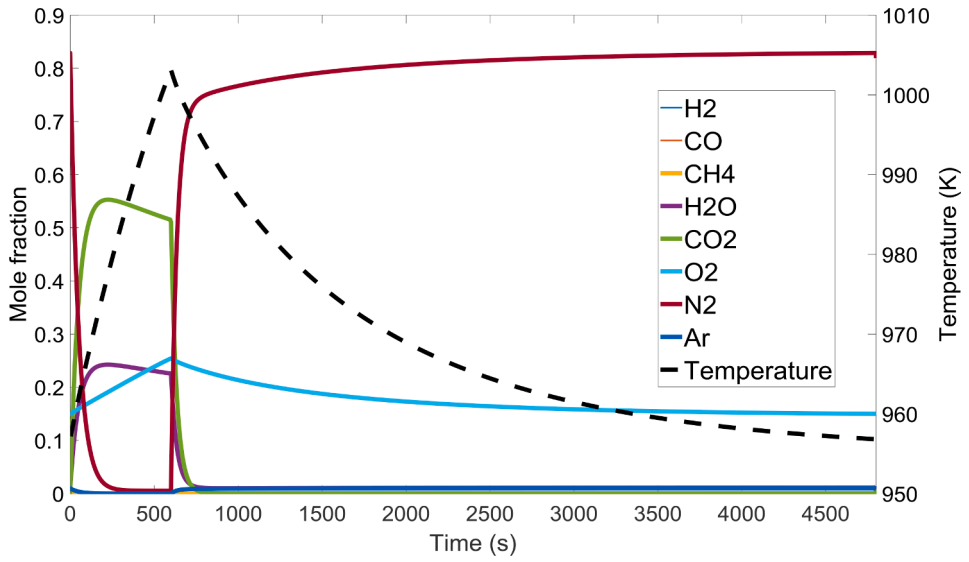

Fig. 19. Reactor outlet gas species composition and temperature plot over a complete GSOP cycle with oxygen production. The first 600 s is the reduction where free oxygen is released in the fuel stream outlet, followed by a long oxidation step (4900 s).

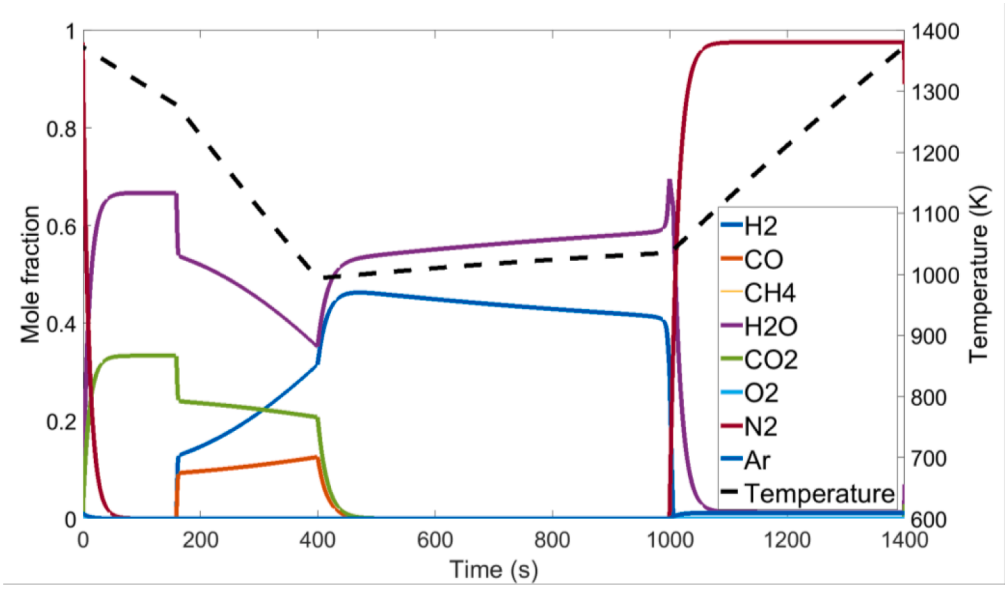

Fig. 20. Reactor outlet gas species composition and temperature plot over a complete GSWS cycle with hydrogen production. The first 400 s is the fuel step where the CH_4 feed is first converted to CO_2 and H_2O, and after 180 s a fuel slip (CO, H_2) is observed. The water splitting step until 1000s is followed by an oxidation step to 1400s.

cycle maximizing the reforming stage average temperature (comparatively increasing methane conversion) and thus enhancing H_2 production (S.M. Nazir et al., 2019). The temperature and composition of the outlet gases from different steps in a GSR cycle is presented in Fig. 16:

3.1.3. Partial oxidation

Gas Switching Partial Oxidation (GSPOX) is an alternative oxygen carrier based on Lanthanum-Iron-Oxide studied for H_2 production applications. Instead of requiring a catalytically active component, this material presents suitable properties for partial oxidation of methane (yielding a H_2 to CO ratio of 2) with very high selectivity (Ugwu et al., 2021). A transition in the reduction step, from full selectivity for H_2O and CO_2), to a partial oxidation stage is observed: selectivity to H_2 and CO in the latter was above 95%, allowing eventually to carry out the reoxidation of the carrier with a steam sweep to produce a relatively pure H_2 stream. A detailed reactor modelling study is presented by

Table 5
Key Performance Indicators definition.

Item	Definition	Units
Electrical Efficiency	$\eta_{el} = \frac{\dot{W}_{net}}{\dot{m}_f LHV_f}$	%
H_2 Equivalent Efficiency	$\eta_{H_2} = \frac{\dot{m}_{H_2} LHV_{H_2}}{\dot{m}_{NG} LHV_{NG} - \frac{\dot{W}_{net}}{\eta_{el,ref}} - \frac{\dot{Q}_{th}}{\eta_{th,ref}}}$	%
CO_2 Avoidance (power)	$CA = \frac{E_{CO_2,ref} - E_{CO_2,CCS}}{E_{CO_2 ref}}$	%
Equivalent CO_2 Capture Ratio (hydrogen)	$CCR_{eq} = \frac{\dot{m}_{CO_2,capt.}}{E_{NG}\dot{m}_{NG} LHV_{NG} - E_{th}\dot{Q}_{th} - E_{el}\dot{W}_{net}}$	%
Levelized Cost of Product	$NPV = \sum_{t=0}^{n} \frac{ACF_t}{(1+i)^t}$	€/unit of P
Cost of CO_2 Avoided	$\frac{ACF_t = \phi \cdot LCOP \cdot P^y - C_{CAPEX} - C_{FOM} - C_{VOM}}{LCOE_{CCS} - LCOE_{ref}}$ $E_{CO_2 ref} - E_{CO_2,CCS}$	€/ton

Arnaiz et al. (Pozo et al., 2021). A GSPOX cycle is shown in Fig. 17, where a two-stage partial oxidation step of a methane fuel is followed by oxidation with air and a reduction step (with full selectivity to H_2O and CO_2). On the other hand, Fig. 18 presents a GSPOX cycle with a water splitting step after partial oxidation of fuel, where only steam is fed to the reactor, yielding a semi pure H_2 stream at the outlet. This feature enables GSPOX clusters to be more effectively coupled to a power cycle, where the H_2 from this step is used for added firing of the oxidation outlet.

3.1.4. Oxygen production

Gas Switching Oxygen Production (GSOP) utilizes an oxygen carrier material capable of releasing free O_2 during the reduction step, which can be subsequently used for oxy-combustion or gasification of solid fuel. The kinetic and reactor modelling of the GSPOP cluster is based on the experimental results provided in (Larring et al., 2017). A GSPOX cycle is presented in Fig. 19, where the O_2 fraction equilibrium composition in the reduction step is observed.

Despite the low development prospects for these materials, several plant configurations integrating this cluster were developed assuming idealized performance of the oxygen carrier (C.A. del Pozo et al., 2019).

3.1.5. Water splitting

Although Gas Switching water splitting was not finally evaluated for large-scale process concepts, due to the low feasibility and performance shown during the materials development phase (Section **0**), a theoretical reactor profile is presented in Fig. 20. Iron oxide is used in a two-stage fuel step, one of complete combustion of methane and a second one with CO/H_2 fuel slip, followed by the water splitting step and final oxidation with air. The equilibrium behaviour of the GSWS process is defined by the reactor temperature, maximizing H_2 yield at low water splitting temperatures. The GSWGS oxygen carrier is of particular interest as it can act as a GSR, when the water splitting step is omitted.

3.2. Power plant techno-economic assessment

A stationary process simulator (Aspen, Unisim Design and/or Thermoflex) was used to synthesize the different power and H_2 plant concepts developed. Average values of flow, composition and temperature of each reaction step from the transient model are provided as input to the stationary process flowsheet. Adequate sizing of the cluster was performed to ensure that variations of properties with respect to the average were relatively small, allowing the safe operation of downstream equipment. Such integration was made automatic through a CAPE-OPEN unit operation, which transferred directly the transient model output to the stationary plant streams. Key performance indicator definitions are provided in Table 5 in the Appendix.

3.2.1. Base-load power plants from solid fuels

The efficiency of base-load power production from solid fuels can be maximized through gasification to produce a syngas fuel, suitable for an F-class gas turbine employed in these models (Anantharaman et al., 2011). As shown in Fig. 21, replacing the combustion chamber with a GSC cluster in an Integrated Gasification Combined Cycle (IGCC) plant employing Hot Gas Clean-Up (HGCU) technology for syngas desulphurization (Giuffrida et al., 2010) yielded very attractive results, with an increase in thermal efficiency of 5.6%-points relative to pre-combustion CO_2 capture reference plant with Selexol absorption, and a 3.3%-points higher CO_2 avoidance (GSC in Fig. 15). On the other hand, efficiency can be boosted above the Unabated IGCC benchmark by around 2%-points when extra firing with natural gas of the O_2 depleted air stream after the GSC is carried out (GSC-AF), at the cost of 10.7%-points lower CO_2 avoidance (C.A. del Pozo et al., 2019). Alternative concepts utilizing GSOP cluster, Oxygen Production Pre-combustion Plant (OPPC) (C.A. del Pozo et al., 2019) and GSC-GSOP IGCC plant (Arnaiz del Pozo et al., 2020), show small energy penalties of approximately 1.3%-points. However, CO_2 avoidance is reduced by around 5%-points, relative to the pre-combustion capture benchmark. Finally, a flexible concept that

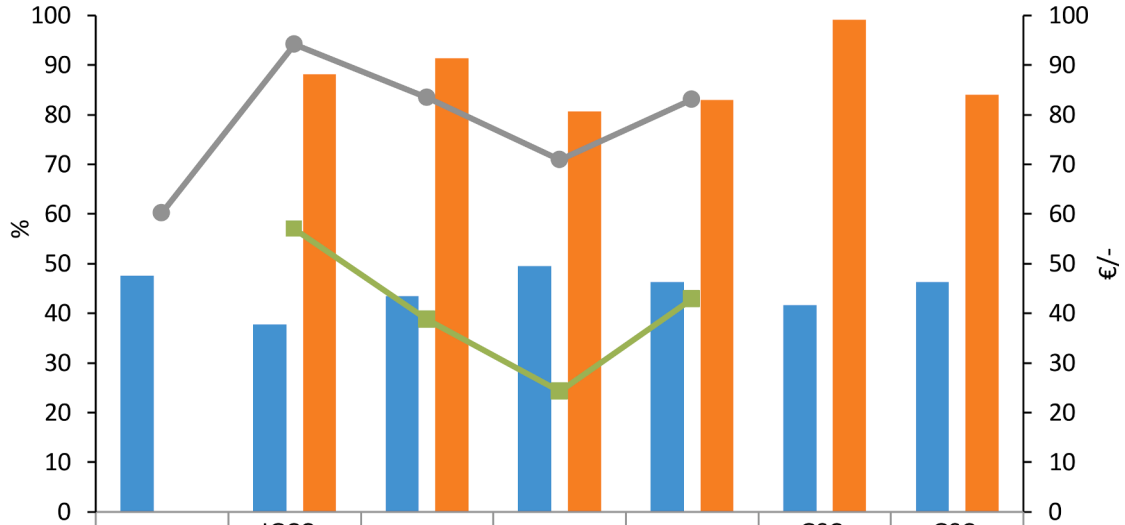

	IGCC	IGCC - PCC	GSC	GSC-AF	OPPC	GSC-HAT	GSC-GSOP
ηEl. (%)	47.6	37.8	43.4	49.5	46.3	41.6	46.3
CA (%)	0	88.1	91.4	80.7	83	99.1	84
LCOE (€/MWh)	60.2	94.2	83.4	70.9	83		
COCA (€/ton)	0	57	38.7	24.3	42.8		

Fig. 21. Electrical efficiency, CO_2 avoidance, levelized cost of electricity and cost of CO_2 avoided results for base-load power plants from solid fuels.

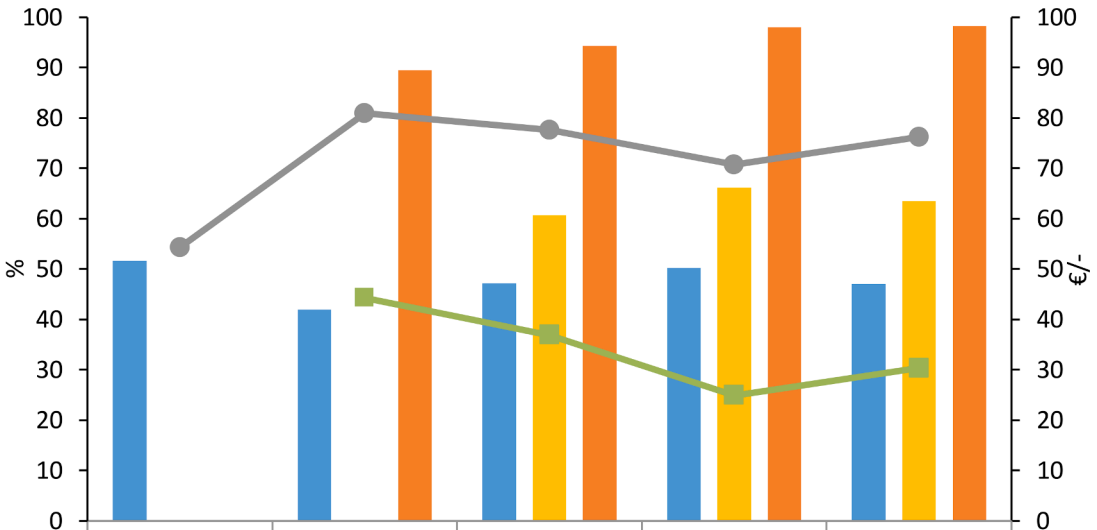

	IGCC	IGCC - PCC	GSC - Shell	GSC - HTW	GSC - GE
ηEl. (%)	51.6	41.9	47.2	50.3	47.1
ηH2 (%)	0	0	60.7	66.2	63.5
CA (%)	0	89.5	94.3	98	98.3
LCOE (€/MWh)	54.3	80.9	77.6	70.7	76.2
COCA (€/ton)	0	44.3	36.9	24.9	30.3

Fig. 22. Electrical and equivalent H_2 efficiency, CO_2 avoidance, levelized cost of electricity and cost of CO_2 avoided results for flexible power plants from solid fuels.

employs the GSC cluster as an energy storage mechanism through decoupling reduction and oxidation sections of the plant, employs a humid air turbine power cycle (Pozo et al., 2020), and achieves 3.8%-points higher thermal efficiency than the pre-combustion CO_2 capture reference, with above 99% CO_2 avoidance (GSC—HAT in Fig. 15).

With regards to the main economic indicators, the conventional pre-combustion capture plant has the highest LCOE, followed by the GSC and OPPC plants that return almost identical LCOE. Added NG firing (GSC-AF) strongly reduces the LCOE by 12.5 €/MWh relative to the standard GSC plant. The gasifier has the highest cost in all cases followed by the gas turbine and the Air Separation Unit (ASU) or GSC unit in the GSC and GSC-AF cases. The gasifier cost is an important uncertainty in the estimation of the OPPC cost. The OPPC plant suffers from a very high gasifier cost due to the syngas flowrate that is more than double the size of the other plants. This high syngas flowrate also increases the gas

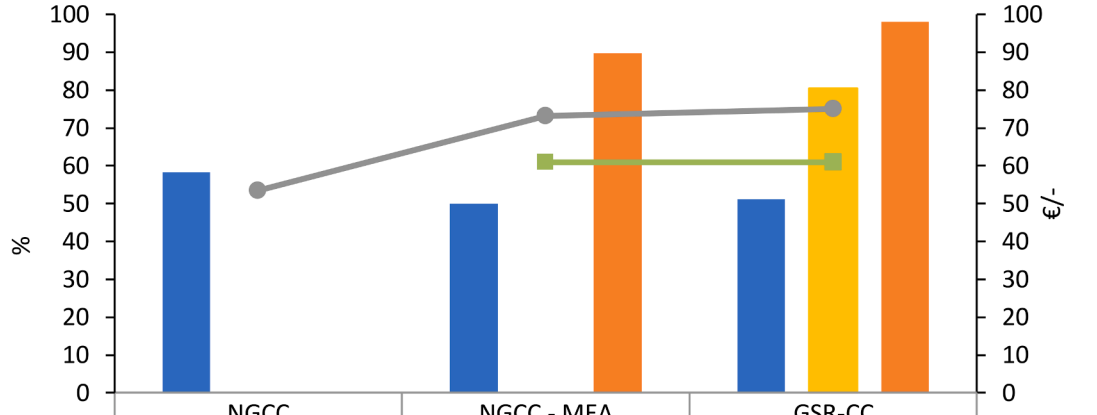

	NGCC	NGCC - MEA	GSR-CC
ηEl. (%)	58.3	49.9	51.1
ηH2 (%)	0	0	80.5
CA (%)	0	89.7	98.1
LCOE (€/MWh)	53.4	73.2	75
COCA (€/ton)	0	60.9	60.9

Fig. 23. Electrical and equivalent H_2 efficiency, CO_2 avoidance, levelized cost of electricity and cost of CO_2 avoided results for flexible power plants from gaseous fuels.

clean-up cost. For perspective, the LCOE of this case reduces to 78.91 €/MWh if the gasifier costs are scaled only by the thermal input and increases to 87.09 €/MWh if scaled only by the raw syngas flowrate. Trends in the COCA indicators are similar to LCOE, although the COCA of the GSC-AF and OPPC plants are increased by their higher CO_2 emissions intensities.

3.2.2. *Flexible power/H_2 plant from solid fuels*

As an enhancement relative to the plants presented in the preceding section, power plant concepts utilizing advanced H-class turbines were developed (C.A. del Pozo et al., 2020). Additionally, the benchmark plants incorporate the benefits derived from HGCU. On the other hand, integration of the GSC clusters and Membrane Assisted Water Gas Shift (MAWGS) reactors (Tosti et al., 2008) allow flexible generation of H_2 at low electricity prices, whereas in favourable market conditions, this H_2 is used for extra firing of the GSC oxidation step outlet, to reach the Combustor Outlet Temperature (COT) of the advanced gas turbine. In Fig. 22, the main results for the advanced GSC IGCC plants and suitable benchmarks are provided. A schematic diagram of these power plant concepts is provided in Fig. 25 in the Appendix. The concepts investigated (GSC-Shell, GSC—HTW, GSC-GE) employ a Shell, High Temperature Winkler and GE gasifiers, leading to an energy penalty reduction of 5.3, 8.4 and 5.2%-points respectively, and a CO_2 avoidance which is 4.8, 8.5 and 8.8%-points higher, relative to the advanced pre-combustion CO_2 capture reference plant (IGCC-PCC). When the plant operates in H_2 production mode, H_2 efficiencies surpassing 60% are attained in all cases.

In terms of economic performance for baseload power production, the LCOE obtained for the two reference cases (without and with CO_2 capture, respectively) shows the benefits offered by the advanced gas turbine and HGCU technology. These cases returned LCOE values of 54.28 and 80.89 €/MWh (Fig. 22) compared to 63.4 and 95.3 €/MWh for the less advanced plants in Fig. 21. The GSC plants achieve a cost of CO_2 avoidance in the range of 24.9 and 36.9 €/ton, lower than for the IGCC-PCC benchmark (44.3 €/ton). The GSC—HTW configuration has the highest efficiency and the lowest capital costs, which reduces LCOE by more than 10 €/MWh relative to the benchmark case. These attractive results apply to baseload plants, but when flexible H_2 exports to balance variable renewable energy are accounted for in the evaluation, attractive cash flow returns can be obtained even at CO_2 prices close to zero (Szima et al., 2021). This benefit stems from the fact that these plants can sell electricity at prices that are above average and continue to profitably sell hydrogen during times when prices are below average.

3.2.3. *Flexible power/H_2 plant from gaseous fuels*

GSR cluster offers the possibility to integrate H_2 production in a combined power cycle, as depicted in Fig. 26 in the Appendix. Similar to the solid fuel plants in the previous section, electricity can be generated through a hydrogen gas-fired combined cycle at times of low renewable energy supply, while exporting H_2 when electricity demand is satisfied by wind and solar (S.M. Nazir et al., 2019). Water vapour is condensed from the exhaust gases from the reduction step in GSR resulting in a pure CO_2 stream that can be compressed for storage. Such configuration achieves a similar energy penalty as a post-combustion CO_2 capture natural gas combined cycle (NGCC), but 8.4%-points higher CO_2 avoidance, as shown in Fig. 23. When considering operation in H_2 production mode, equivalent hydrogen production efficiencies surpass 80%, and the plant requires electricity imports (a positive feature given that hydrogen will be exported when electricity prices are low). For standard baseload economic assessment at a capacity factor of 85% revealed that the GSR combined cycle (GSR-CC) power plant has a slightly higher LCOE than the benchmark NGCC plant with MEA post-combustion CO_2 capture (74.95 €/MWh for GSR and 73.18 €/MWh for MEA). However, when the economic benefits of flexible operation are considered, the GSR-CC plant can achieve an attractive 5%-point higher annualized investment return than the NGCC-MEA benchmark (Szima et al., 2019).

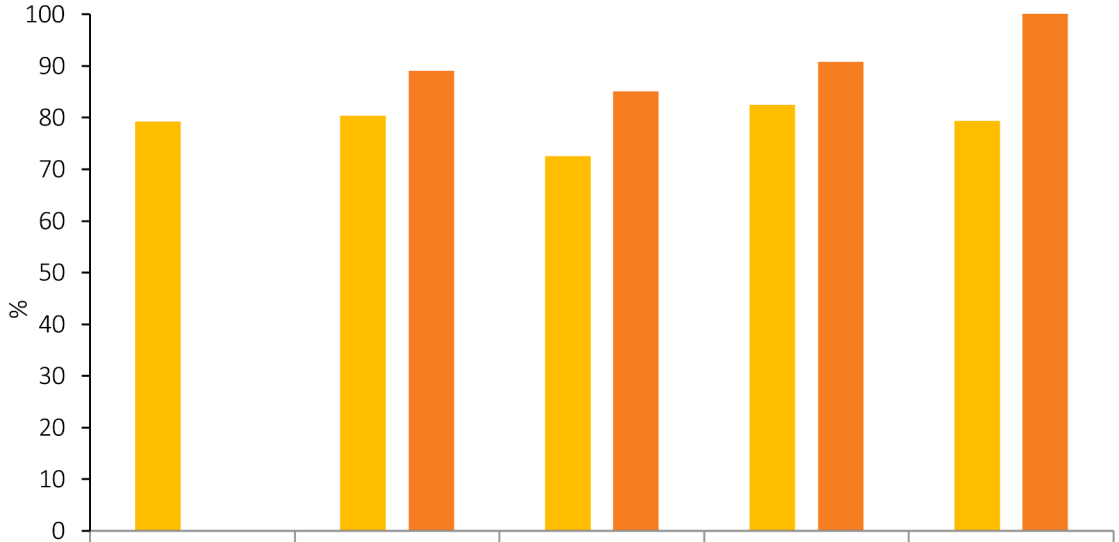

	SMR	GSR H2	SMR MDEA	GSPOX H2	GSPOX H2-Power
ηH2 (%)	79.3	80.4	72.5	82.5	79.4
CCReq (%)	0	89	85.1	90.8	140.4
LCOH (€/kg)	1.71	1.85	0	0	0
COCA (€/ton)	0	18	0	0	0

Fig. 24. Equivalent hydrogen efficiency, equivalent carbon capture ratio, levelized cost of hydrogen and cost of CO_2 avoided for H_2 plants.

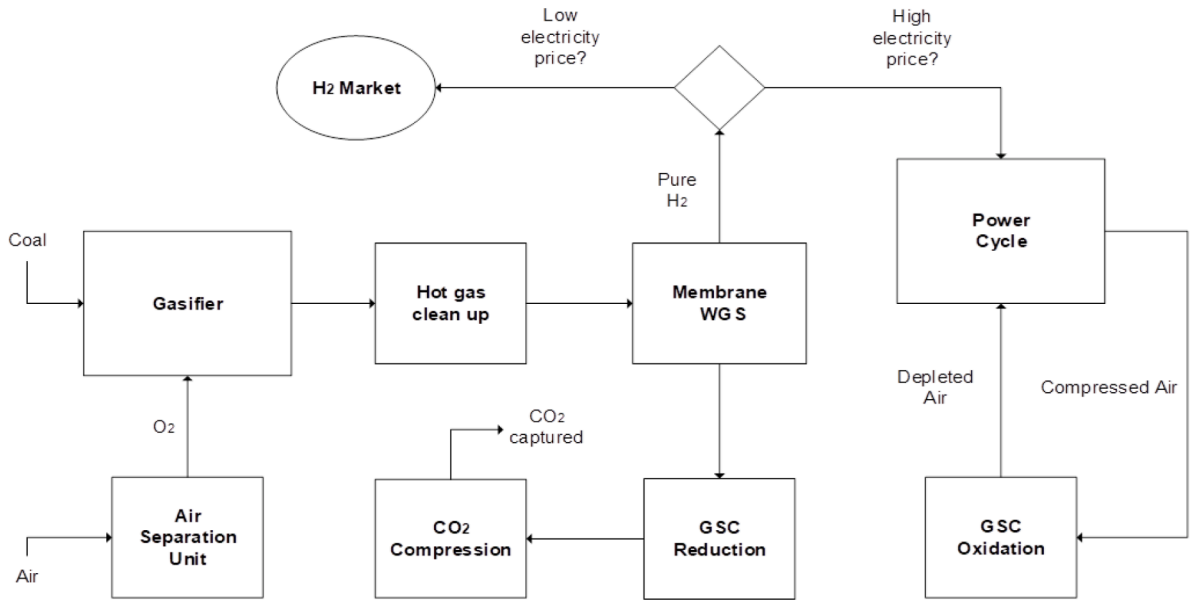

Fig. 25. Block flow diagram of the flexible power/H2 plant from solid fuels.

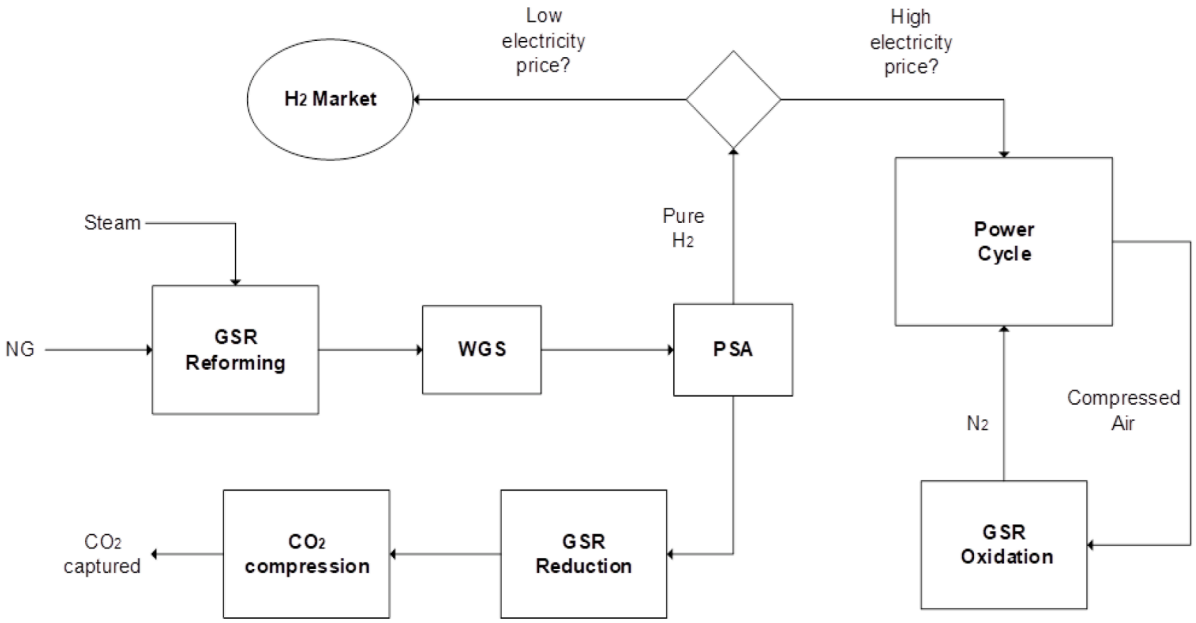

Fig. 26. Block flow diagram of flexible power/H_2 plant from gaseous fuels.

3.3. H_2 plant techno-economic assessment

Due to the resurging interest in the H_2 economy, GS technology was investigated as a potential candidate for "blue" hydrogen production from natural gas, with promising results (S.M. Nazir et al., 2019). The concept entails integrating a GSR cluster with a WGS train, to maximize conversion of CO. After WGS, a PSA unit retrieves a purified H_2 stream as a product and the resulting low heating value off gas is utilized in the GSR cluster reduction step to provide heat for reforming. A compressor delivers air to the oxidation step, while a small turbine retrieves some power. Overall, electricity must be imported to the plant, resulting in a similar H_2 equivalent efficiency as a Steam Methane Reforming (SMR) benchmark without CO_2 abatement, as reflected in Fig. 23 CO2 avoidance is around 4%-points higher than the SMR reference plant with pre-combustion capture with MDEA absorption (SMR MDEA), as shown in Fig. 24. LCOH of the GSR-H_2 plant shows competitive results even when CO_2 taxes are not considered (Nazir et al., 2020). On the other hand, evaluation of the GSPOX carrier showed small performance improvements relative to GSR, primarily due to a better heat recuperation, and to smaller steam to carbon demand of the GSPOX (case GSPOX-H_2). Operating pressure increase mildly benefited GSPOX relative to GSR (Pozo et al., 2021). When the GSPOX cluster was integrated into an advanced power cycle to produce electricity and H_2 (GSPOX H_2-power), the equivalent efficiency results comparable to the SMR unabated benchmark, but CO_2 avoidance of more than 140% was reached, due to clean electricity exports avoiding emissions incurred in the reference unabated NGCC electricity generation plant.

4. Conclusion

Chemical looping processes (combustion, reforming, water splitting, oxygen production, and partial oxidation of methane) have been studied using the novel Gas Switching Technology. Although the GST has been successfully demonstrated, further research is still needed to ensure feasible scale-up and commercialization as outlined below:

- For the reforming demonstration, Ni was only partially substituted and not eliminated to achieve a completely safe operation for scale-up and commercialization of the GSR concept. This calls for more research to develop non-toxic and affordable oxygen carriers to actualize the full GSR potential and ensure that human health would not be put at risk during scale-up and commercialization. The maximum pressure achieved for the GSR demonstration is 5 bar, therefore operation at higher pressures should also be completed.
- The demonstration of CO_2 utilization through Gas Switching Dry Reforming (GSDR) suggests that there could be enormous benefits in integrating GSDR into GTL processes. It is therefore important to optimize the GSDR process and demonstrate further at higher pressures close to the target downstream GTL processes.
- The operation of GSWS is still not optimal due to excessive gas mixing with the 35 wt.% Fe_2O_3/Al_2O_3 in the 1st demonstration. The 2nd demonstration with 74 wt.% active content Cu-doped Mg $(Fe_{0.9}Al_{0.1})_2O_4$ spinel oxygen carrier created three operational challenges that should be addressed in future work to increase the attractiveness of the GSWS concept. Alternatively, a downstream pressure swing adsorption unit can be used to purify the H_2 before utilization.
- Although the GSPOX process was also demonstrated at high pressure with over 70% fuel conversion achieved at 5 bar and 950 °C, further demonstrations for continuous operation at higher pressures are required to improve the process efficiency and achieve an easy integration into downstream GTL processes which always operate a high pressure up from 30 bar.
- A comprehensive reactor modelling, process modelling, and techno-economics are required for the GSWS, GSDR and GSPOX processes to provide a more fundamental explanation of the process behaviour, ascertain the economic viability, and the possibility for scale-up. The proposed GST technology should be benchmarked with other similar technologies (such as the gas switching chemical looping technology using a fixed bed reactor) to ascertain its comparative advantages.
- With the successful demonstrations of the reactor cluster for Auto-thermal GSC operation, a pilot-scale plant is required to test all the process value chains for commercialization followed by a comprehensive business case based on pilot demonstrations.

The techno-economic assessment studies for electricity and H_2 production carried out in the project employing simplified dynamic cluster models and stationary process simulation tools reveal attractive prospects for several GST technologies. GSR integration into a NGCC as a load following plant offers the possibility to balance variable renewable energy while delivering a carbon-free energy vector (H_2) at times when energy supply is guaranteed by wind and solar, maximizing capital utilization. On the other hand, GSR integration for base-load H_2 production from natural gas presents a comparable equivalent efficiency to an unabated SMR plant whilst achieving an equivalent carbon capture of approximately 90%, showcasing a compelling "blue H_2" process. Furthermore, integration of GSC clusters and high-temperature syngas contaminant removal in gasification plants for base-load power production from solid fuels result in substantial economic gains relative to conventional CO_2 capture technologies. Flexibility to produce H_2 or electricity depending on market conditions can be achieved through integration membrane reactors, albeit at significantly increasing plant complexity. To further enhance the interest in the development of GST clusters and suitable oxygen carrier materials, it is recommended from a techno-economic assessment angle to carry out future evaluations regarding the integration of GST technology in hybrid power-chemical production plants (such as ammonia, methanol, GtL), with a particular emphasis on flexibility and product diversification, providing energy vectors which are more easily stored and transported than H_2. Such features will become a key competitive aspect for fossil fuelled-based plants in an energy scenario with a high renewable penetration.

Declaration of Competing Interest

None

Acknowledgement

ACT GaSTech project. Project No 271511.

This project has received funding from The Research Council of Norway and is cofounded by the European Commission under the Horizon 2020 program, ACT Grant Agreement No 691712. It also received the 2019 Equinor Publication Grant. VATL Lab technicians at the Norwegian University of Science and Technology are equally acknowledged for constructing and maintaining the experimental setup. The partners collaborating in this project also received funding from MINECO, Spain (reference PCIN-2017–013).

Appendix

GS technology kinetic expressions

Key performance Indicators

$\dot{W}_{net}$ indicates net electric export/import, $\dot{m}$ is the flowrate, *LHV* is the lower heating value and *ref* refers to a reference benchmarking plant. *CA* is the CO_2 avoidance, *E is* the CO_2 intensity of a given plant (producing electricity, steam, H_2) or feedstock (natural gas), *CCS* refers to the plant with carbon capture and storage. $\dot{Q}_{th}$ indicates the steam enthalpy difference from export conditions to saturated liquid. CCR_{eq} stands for equivalent carbon capture ratio. *NPV* stands for net present value of the project, ACF_t is the annual cash flow rate, C_{CAPEX} C_{FOM} C_{VOM} is the cost of capital, fixed and variable operation & maintenance, respectively. ϕ indicates the plant capacity factor, i is the discount rate and t is the operating year. *LCOP* is the levelized cost of product (electricity or H_2), at which the *NPV* becomes 0 at then of the plant lifetime, while P^y refers to the annual production of product.

Flexible plant block flow diagrams

Flexible power/H_2 plant from solid fuels

Flexible power/H_2 plant from gaseous fuels

References

Abad, A., et al., 2007. Mapping of the range of operational conditions for Cu-, Fe-, and Ni-based oxygen carriers in chemical-looping combustion. Chem. Eng. Sci. 62 (1–2), 533–549.

Abanades, J.C., et al., 2015. Emerging CO2capture systems. Int. J. Greenhouse Gas Control.

Adánez, J., Abad, A., 2019. Chemical-looping combustion: status and research needs. Proc. Combust. Inst. 37 (4), 4303–4317.

Adanez, J., et al., 2012. Progress in chemical-looping combustion and reforming technologies. Prog. Energy Combust. Sci. 38 (2), 215–282.

Anantharaman, R., et al., 2011. DECARBit: European Best Practice Guidelines For Assessment of CO2 Capture Technologies. Norwegian University of Science and Technology, Trondheim, Norway.

Arnaiz del Pozo, C., et al., 2020a. Exergy analysis of gas switching chemical looping IGCC plants. Energies 13 (3), 544.

Arnaiz del Pozo, C., et al., 2020b. Integration of gas switching combustion in a humid air turbine cycle for flexible power production from solid fuels with near-zero emissions of CO2 and other pollutants. Int. J. Energy Res. 44 (9), 7299–7322.

Bischi, A., et al., 2011. Design study of a 150 kWth double loop circulating fluidized bed reactor system for chemical looping combustion with focus on industrial applicability and pressurization. Int. J. Greenhouse Gas Control 5 (3), 467–474.

Chen, L., et al., 2018. Pressurized chemical looping combustion for solid fuel. Handbook Chem. Looping Technol. 123–158.

Cloete, S., et al., 2015. Integration of a Gas Switching Combustion (GSC) system in integrated gasification combined cycles. Int. J. Greenhouse Gas Control 42, 340–356.

Cloete, S., et al., 2016. Gas switching as a practical alternative for scaleup of chemical looping combustion. Energy Technol. 4 (10), 1286–1298.

Cloete, S., et al., 2017. Optimization of a Gas Switching Combustion process through advanced heat management strategies. Appl. Energy 185, 1459–1470.

del Pozo, C.A., et al., 2019a. The potential of chemical looping combustion using the gas switching concept to eliminate the energy penalty of CO2 capture. Int. J. Greenhouse Gas Control 83, 265–281.

del Pozo, C.A., et al., 2019b. The oxygen production pre-combustion (OPPC) IGCC plant for efficient power production with CO2 capture. Energy Convers. Manage. 201, 112109.

del Pozo, C.A., et al., 2020a. Exergy analysis of gas switching chemical looping IGCC plants. Energies 13 (3), 1–25.

del Pozo, C.A., et al., 2020b. Integration of gas switching combustion and membrane reactors for exceeding 50% efficiency in flexible IGCC plants with near-zero CO2 emissions. Energy Convers. Manag. 7, 100050.

Donat, F., Müller, C.R., 2020. CO2-free conversion of CH4 to syngas using chemical looping. Appl. Catal. B 278, 119328.

Donat, F., Xu, Y., Müller, C.R., 2020. Combined partial oxidation of methane to synthesis gas and production of hydrogen or carbon monoxide in a fluidized bed using lattice oxygen. Energy Technol. 8 (8), 1900655.

Fisher, J.C., Siriwardane, R.V., Stevens Jr, R.W., 2012. Process for CO2 capture from high-pressure and moderate-temperature gas streams. Ind. Eng. Chem. Res. 51 (14), 5273–5281.

Giuffrida, A., Romano, M.C., Lozza, G.G., 2010. Thermodynamic assessment of IGCC power plants with hot fuel gas desulfurization. Appl. Energy 87 (11), 3374–3383.

Hallberg, P., et al., 2016. Investigation of a calcium manganite as oxygen carrier during 99h of operation of chemical-looping combustion in a 10 kWth reactor unit. Int. J. Greenhouse Gas Control 53, 222–229.

Hamers, H.P., et al., 2014. Comparison on process efficiency for CLC of syngas operated in packed bed and fluidized bed reactors. Int. J. Greenhouse Gas Control 28 (0), 65–78.

Hamers, H.P., et al., 2015. Experimental demonstration of CLC and the pressure effect in packed bed reactors using NiO/CaAl2O4 as oxygen carrier. Fuel 159, 828–836.

IEA World Energy Outlook report. 2021.

Larring, Y., et al., 2017. COMPOSITE: a concept for high efficiency power production with integrated CO2 capture from solid fuels. Energy Procedia 114, 539–550.

Luis, F., et al., 2009. Hydrogen production by chemical-looping reforming in a circulating fluidized bed reactor using Ni-based oxygen carriers. J. Power Sources 192 (1), 27–34.

Lyngfelt, A., et al., 2019. 11,000h of chemical-looping combustion operation—where are we and where do we want to go? Int. J. Greenhouse Gas Control 88, 38–56.

Lyngfelt, A., 2013. Chemical Looping Combustion (CLC), in Fluidized bed Technologies For Near-Zero Emission Combustion and Gasification. Elsevier, pp. 895–930.

Mattisson, T., et al., 2014. Innovative oxygen carriers uplifting chemical-looping combustion. Energy Procedia 63, 113–130.

Nazir, S.M., et al., 2018. Techno-economic assessment of the novel gas switching reforming (GSR) concept for gas-fired power production with integrated CO2 capture. Int. J. Hydrogen Energy 43 (18), 8754–8769.

Nazir, S.M., et al., 2019a. Efficient hydrogen production with CO2 capture using gas switching reforming. Energy.

Nazir, S.M., et al., 2019b. Efficient hydrogen production with CO2 capture using gas switching reforming. Energy 185, 372–385.

Nazir, S.M., et al., 2019c. Gas switching reforming (GSR) for power generation with CO2 capture: process efficiency improvement studies. Energy 167, 757–765.

Nazir, S.M., et al., 2020. Pathways to low-cost clean hydrogen production with gas switching reforming. Int. J. Hydrogen Energy.

Noorman, S., Annaland, M.V., Kuipers, H., 2007. Packed bed reactor technology for chemical-looping combustion. Ind. Eng. Chem. Res. 46 (12), 4212–4220.

Noorman, S., van Sint Annaland, M., Kuipers, J., 2010. Experimental validation of packed bed chemical-looping combustion. Chem. Eng. Sci. 65 (1), 92–97.

Osman, M., et al., 2019. Internally circulating fluidized-bed reactor for syngas production using chemical looping reforming. Chem. Eng. J. 377, 120076.

Osman, M., et al., 2020. Experimental demonstration of pressurized chemical looping combustion in an internally circulating reactor for power production with integrated CO2 capture. Chem. Eng. J. 401, 125974.

Osman, M., et al., 2021. Review of pressurized chemical looping processes for power generation and chemical production with integrated CO2 capture. Fuel Process. Technol. 214, 106684.

Pozo, A.d., et al., 2021. The potential of gas switching partial oxidation using advanced oxygen carriers for efficient H2 production with inherent CO2 capture. Applied Sci. (Under Review).

Rydén, M., Arjmand, M., 2012. Continuous hydrogen production via the steam–iron reaction by chemical looping in a circulating fluidized-bed reactor. Int. J. Hydrogen Energy 37 (6), 4843–4854.

Science, N.M.F. Chemical Looping Combustion. [cited 2019 June]; Available from: https://mfix.netl.doe.gov/research/chemical-looping-combustion/.

Spallina, V., et al., 2017. Chemical looping reforming in packed-bed reactors: modelling, experimental validation and large-scale reactor design. Fuel Process. Technol. 156, 156–170.

Szima, S., et al., 2019. Gas switching reforming for flexible power and hydrogen production to balance variable renewables. Renewable Sustainable Energy Rev. 110, 207–219.

Szima, S., et al., 2021. Finding synergy between renewables and coal: flexible power and hydrogen production from advanced IGCC plants with integrated CO2 capture. Energy Convers. Manage. 231, 113866.

Tosti, S., et al., 2008. Design and process study of Pd membrane reactors. Int. J. Hydrogen Energy 33 (19), 5098–5105.

Ugwu, A., et al., 2019a. Gas Switching Reforming for syngas production with iron-based oxygen carrier-the performance under pressurized conditions. Int. J. Hydrogen Energy.

Ugwu, A., Zaabout, A., Amini, S., 2019b. An advancement in CO2 utilization through novel gas switching dry reforming. Int. J. Greenhouse Gas Control 90, 102791.

Ugwu, A., et al., 2020a. Gas Switching Reforming for syngas production with iron-based oxygen carrier-the performance under pressurized conditions. Int. J. Hydrogen Energy 45 (2), 1267–1282.

Ugwu, A., et al., 2020b. Hydrogen production by water splitting using gas switching technology. Powder Technol. 370, 48–63.

Ugwu, A., et al., 2021. Combined Syngas and Hydrogen Production using Gas Switching Technology. Ind. Eng. Chem. Res. 60 (9), 3516–3531.

Voitic, G., Hacker, V., 2016. Recent advancements in chemical looping water splitting for the production of hydrogen. RSC Adv. 6 (100), 98267–98296.

Wang, P., et al., 2015. Chemical-looping combustion and gasification of coals and oxygen carrier development: a brief review. Energies 8 (10), 10605–10635.

Wassie, S.A., et al., 2017a. Hydrogen production with integrated CO2 capture in a novel gas switching reforming reactor: proof-of-concept. Int. J. Hydrogen Energy 42 (21), 14367–14379.

Wassie, S.A., et al., 2017b. Hydrogen production with integrated CO2 capture in a novel gas switching reforming reactor: proof-of-concept. Int. J. Hydrogen Energy 42 (21), 14367–14379.

Wassie, S.A., et al., 2017c. Detecting densified zone formation in membrane-assisted fluidized bed reactors through pressure measurements. Chem. Eng. J. 308, 1154–1164.

Wassie, S.A., et al., 2017d. Hydrogen production with integrated CO2 capture in a novel gas switching reforming reactor: Proof-Of-Concept 42 (21), 14367–14379.

Wassie, S.A., et al., 2018a. Techno-economic assessment of membrane-assisted gas switching reforming for pure H2 production with CO2 capture. Int. J. Greenhouse Gas Control 72, 163–174.

Wassie, S.A., et al., 2018b. Hydrogen production with integrated CO2 capture in a membrane assisted gas switching reforming reactor: proof-of-Concept. Int. J. Hydrogen Energy 43 (12), 6177–6190.

Wassie, S.A., et al., 2016. The effect of gas permeation through vertical membranes on chemical switching reforming (CSR) reactor performance. Int. J. Hydrogen Energy 41 (20), 8640–8655.

Xiao, R., et al., 2012. Pressurized chemical-looping combustion of coal using an iron ore as oxygen carrier in a pilot-scale unit. Int. J. Greenhouse Gas Control 10, 363–373.

Xu, J., Froment, G.F., 1989. Methane steam reforming, methanation and water-gas shift: I. Intrinsic kinetics. AlChE J. 35 (1), 88–96.

Zaabout, A., et al., 2013a. Experimental demonstration of a novel gas switching combustion reactor for power production with integrated CO2 capture. Ind. Eng. Chem. Res. 52 (39), 14241–14250.

Zaabout, A., et al., 2013b. Experimental demonstration of a novel gas switching combustion reactor for power production with integrated CO2 capture. Ind. Eng. Chem. Res. 52 (39), 14241–14250.

Zaabout, A., et al., 2015. A novel gas switching combustion reactor for power production with integrated CO2 capture: sensitivity to the fuel and oxygen carrier types. Int. J. Greenhouse Gas Control 39, 185–193.

Zaabout, A., Cloete, S., Amini, S., 2016a. Innovative Internally Circulating Reactor Concept for Chemical Looping-Based CO2 Capture Processes: hydrodynamic Investigation. Chem. Eng. Technol. 39 (8), 1413–1424.

Zaabout, A., et al., 2016b. Experimental demonstration of control strategies for a Gas Switching Combustion reactor for power production with integrated CO2 capture. Chem. Eng. Res. Des. 111, 342–352.

Zaabout, A., Cloete, S., Amini, S., 2017. Autothermal operation of a pressurized Gas Switching Combustion with ilmenite ore. Int. J. Greenhouse Gas Control 63, 175–183.

Zaabout, A., et al., 2018. A pressurized gas switching combustion reactor: autothermal operation with a CaMnO3− δ-based oxygen carrier. Chem. Eng. Res. Des. 137, 20–32.
Zaabout, A., et al., 2019. Gas Switching Reforming (GSR) for syngas production with integrated CO2 capture using iron-based oxygen carriers. Int. J. Greenhouse Gas Control 81, 170–180.
ZAABOUT, A., S. CLOETE, and S. AMINI, Autothermal operation of a pressurized gas switching combustion reactor with a Mn-based oxygen carrier. 2021.
Zhang, S., Xiao, R., Zheng, W., 2014. Comparative study between fluidized-bed and fixed-bed operation modes in pressurized chemical looping combustion of coal. Appl. Energy 130, 181–189.